ACS Biomaterials SCIENCE & ENGINEERING

pubs.acs.org/journal/abseba

Review

Poly(aspartic acid) in Biomedical Applications: From Polymerization, Modification, Properties, Degradation, and Biocompatibility to Applications

Hossein Adelnia, Huong D.N. Tran, Peter J. Little, Idriss Blakey, and Hang T. Ta*

Cite This: https://doi.org/10.1021/acsbiomaterials.1c00150

Read Online

ACCESS | Metrics & More | Article Recommendations

ABSTRACT: Poly(aspartic acid) (PASP) is an anionic polypeptide that is a highly versatile, biocompatible, and biodegradable polymer that fulfils key requirements for use in a wide variety of biomedical applications. The derivatives of PASP can be readily tailored via the amine-reactive precursor, poly(succinimide) (PSI), which opens up a large window of opportunity for the design and development of novel biomaterials. PASP also has a strong affinity with calcium ions, resulting in complexation, which has been exploited for bone targeting and biomineralization. In addition, recent studies have further verified the biocompatibility and biodegradability of PASP-based polymers, which is attributed to their protein-like structure. In light of growing interest in PASP and its derivatives, this paper presents a comprehensive review on their synthesis, characterization, modification, biodegradation, biocompatibility, and applications in biomedical areas.

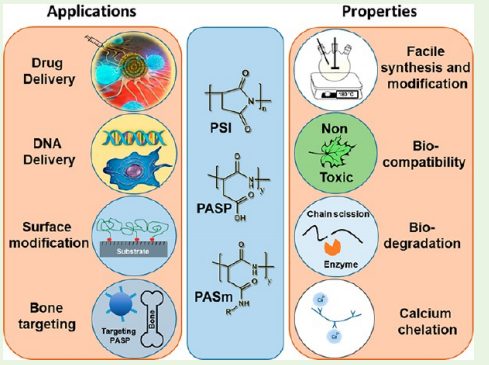

KEYWORDS: *poly(aspartic acid), poly(succinimide), synthesis and characterizations, biodegradation, biomedical applications*

1. INTRODUCTION

Polyelectrolytes are an important class of water-soluble polymers that have a wide variety of applications.[1] Depending on the chemical structure, they can be divided into cationic, anionic, and zwitterionic. The charged species along the chain in polyelectrolytes endow them with interesting features such as pH- and ionic-sensitivity. Anionic polymers are a widely used class of polyelectrolytes thanks to the presence of acidic groups in the backbone.[2] Upon increasing pH, the chain conformation changes from globular to a coil, adopting an extended state. Extensive research has been conducted by exploiting this conformational change.[3]

The majority of anionic polymers such as poly(acrylic acid) (PAA), though well-established and effective, are not readily degradable.[4] Thus, the need to seek and develop a viable alternative is highly desirable. Poly(amino acids), thanks to their protein-like backbone structure, are ideal substitutes for nondegradable anionic polyelectrolytes. Among them, PASP is a comparatively inexpensive polymer because it can be obtained from poly(succinimide) (PSI) which is easily synthesized by thermal polymerization of commercially available raw materials such as aspartic acid (ASP) or maleamic acid.[5] Moreover, PSI can undergo a ring-opening reaction with primary amine-containing agents in the absence of catalyst at room temperature. Following the alkali hydrolysis of the remaining succinimide units, modified PASP is obtained. Such facile modification with a wide variety of compounds ranging from fluorescent dyes to drugs makes this class of polymers highly versatile and broadly applicable. For instance, it has led to the development of variety of interesting materials for biomedical applications, including tissue engineering and drug/gene delivery.[6]

In addition, the biocompatibility of PASP together with its biodegradability arising from peptide bonds in the backbone makes it even more attractive for biomedical applications.[7,8] PASP also has strong affinity with calcium ions, resulting in the formation of PASP-Ca complexes, which has been exploited for bone targeting and biomineralization.[9−12] The anionic charges along the chain also make PASP a suitable component in polyelectrolyte complexes with a cationic agent (e.g., chitosan). These complexes are referred to as polyelectrolyte bi- or multilayers and was reviewed recently with a considerable emphasis on poly(aspartimide)s as PASP derivatives.[6] Another review was also published in 2018 on the synthesis and modification of PSI and poly(aspartimide) derivatives.[5]

Considering the above-mentioned facts and given the growing demand for an easily synthesizable and modifiable

Received: January 29, 2021
Accepted: March 22, 2021

Scheme 1. Overview of the Properties and Biomedical Applications of Poly(aspartic acid) and its Derivatives

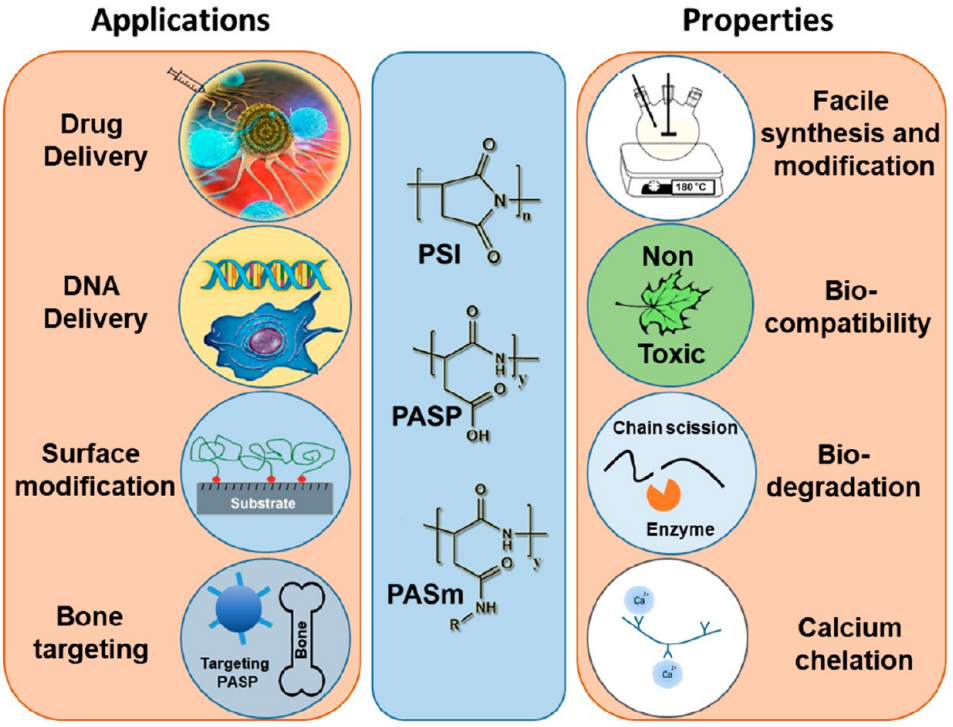

biomaterial, prompted us to present an up-to-date and comprehensive review on the topic with an emphasis on PASP in particular as well as its derivatives in general (Scheme 1). In this paper, different approaches of synthesis, characterization, and modification are summarized. Furthermore, various features of the polymers that benefit their applications in biomedical fields have also been covered.

2. SYNTHESIS

PASP is typically synthesized by polymerization of aspartic acid (ASP) or maleic anhydride as shown in Figure 1a. Both methods are poly condensation reactions and thus elevated temperatures (>160 °C) and byproduct removal (i.e., water) are required for achieving high molecular weights and reaction yields. The product of both reactions is the intermediate poly(anhydroaspartic acid), i.e., PSI, which can be easily hydrolyzed to ring-open the succinimide to form PASP under mild alkaline conditions. Ring-opening can occur through either of the two carbonyls, leading to a combination of α and β configuration in the final product. In addition, in the presence of molecules bearing primary amines, PSI undergoes a nucleophilic reaction under mild conditions without the need for any catalyst (Figure 1a, bottom, right). This reaction yields poly(aspartamide) derivatives, allowing one to yield PASP with a wide variety of species ranging from polymers to drugs.[13−15] Homo- and copolymerization of ASP will be discussed in the following.

2.1. Poly Condensation of ASP. The most common synthesis method of PASP is poly condensation of ASP at elevated temperatures (>160 °C), which is carried out either in bulk or solution, in the presence or absence of a catalyst (Figure 1a left-top). Depending on the reaction parameters, PASP with different yields and molecular weights has been obtained as summarized in Table 1. Low et al.[16] synthesized PASP at 260 °C without any solvent and catalyst at high yield (97%). They found the ratio of α/β to be 0.3/0.7 by ^{13}C NMR and M_w of 5.2 kDa (i.e., g/mol $\times 10^{-3}$) by HPLC. Similarly, other work also revealed that the α:β linkage ratio is 1:3 regardless of the reaction conditions.[17] Furthermore, it was indicated that use of phosphoric acid (H_3PO_4) as a catalyst lowers the extent of chain branching. Tomida et al.[18] investigated the effect of different solvents and found that the mixture of mesitylene/sulfolane (7/3, w/w) gives rise to the highest M_w of 64.3 kDa and yield of 96%. Other examined solvents or mixed solvents such as toluene, DMF,, and toluene/sulfolane were either incapable of or inefficient in giving high yield and molecular weight.

It is worth mentioning that although the solvent facilitates heat transfer, it can lower the rate of reaction because of the decreased concentration of reactive functional groups.[19] In addition, for large scale syntheses, the solvent used needs to be extracted from the product and recovered by difficult and expensive techniques, such as polymer precipitation and solvent evaporation.[20] To facilitate and industrialize the production, Nakato et al.[21] polymerized aspartic acid in the bulk under batch and continuous (using an extruder) conditions in the presence of H_3PO_4 as the catalyst. A M_w of 24 kDa with the rare occurrence of chain scission was achieved. In addition, Zrinyi et al.[22] polymerized aspartic acid with H_3PO_4 as the catalyst both in solution (mesitylene/sulfolane, 16 mol % of H_3PO_4) and bulk (solvent-free, 1:1 w:w, H_3PO_4:aspartic acid) and found that the latter yields much higher molecular weight and viscosity. Although bulk reaction seems less complex in terms of purification and more effective in terms of yield, it was shown that as the reaction temperature was increased from 160 to 200 °C, the optical purity (enantiomeric excess) of PASP decreases continuously.[23] Furthermore, high viscosity and difficult mixing are other challenges for bulk reaction.[21,24]

https://doi.org/10.1021/acsbiomaterials.1c00150
ACS Biomater. Sci. Eng. XXXX, XXX, XXX−XXX

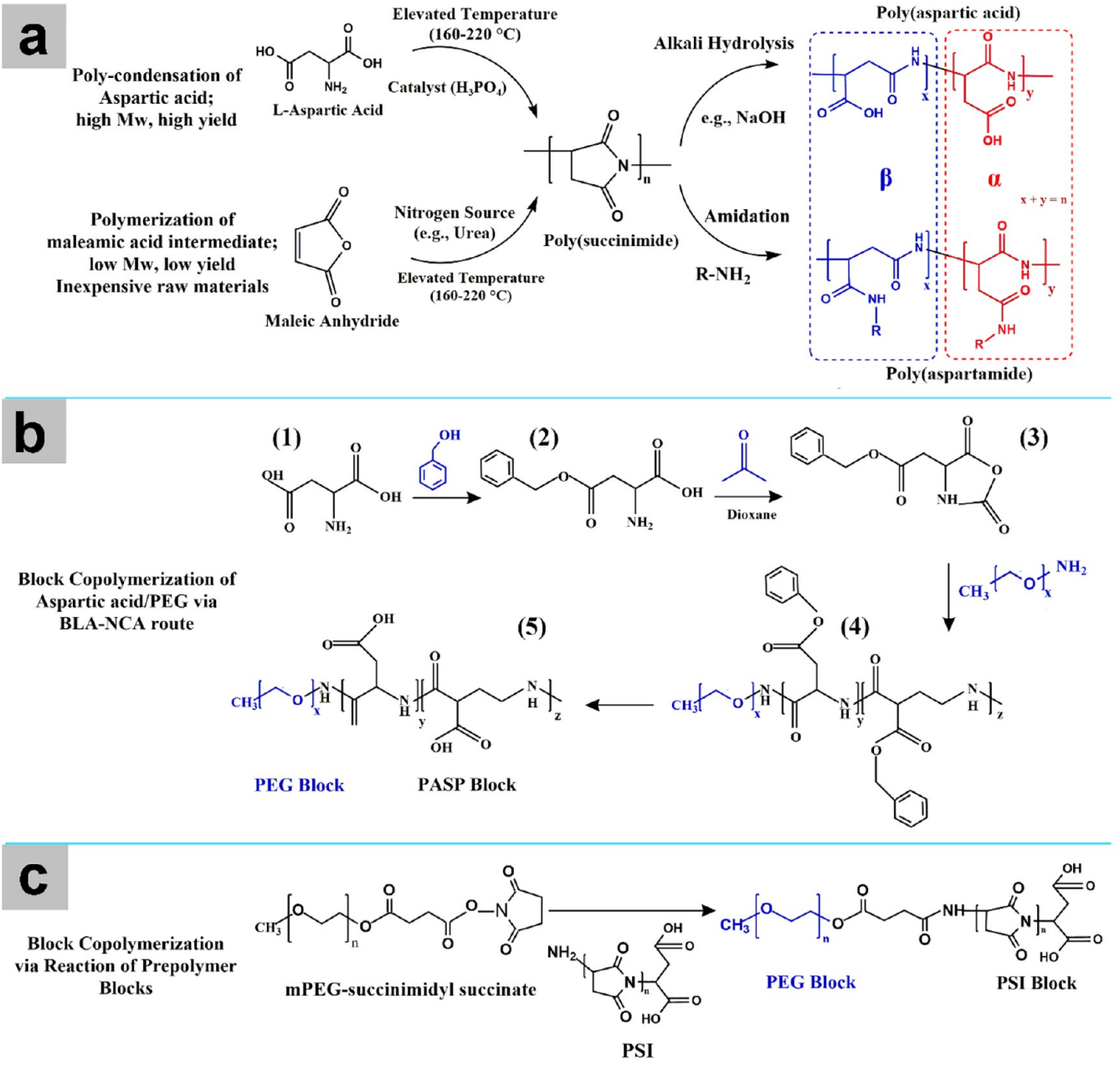

Figure 1. Schematic representations of synthesis, modification, and copolymerization of PASP and its derivatives. (a) Synthesis of the PSI intermediate via poly condensation of ASP at elevated temperature in the presence of phosphoric acid as the most effective catalyst (top panel left). Subsequent hydrolysis of PSI yields PASP with combination of α and β configuration (top panel right). PSI synthesis can be carried out via polymerization of maleamic acid (bottom panel left). PSI can be ring-opened via the application of primary amines (also called amidation reaction) (bottom panel right) (b) Synthetic pathway of PEG-*b*-PASP block copolymer.[46] (c) block copolymerization of PEG and ASP via succinimidyl succinate-capped PEG and PSI prepolymer.[49]

2.2. Polymerization of Maleic Anhydride/Ammonium Salt of Maleic acid. The second method involves the reaction of maleic anhydride (MA) or alternatively maleic acid with a nitrogen source such as urea or ammonia (NH_3), giving rise to maleamic acid. The latter is then reacted at high temperature (>160 °C) in the presence or absence of a catalyst to yield PSI (Figure 1a left-bottom).[31−36] This method was first conducted and patented employing maleic acid and NH_3.[36] The synthesized PASP had a relatively low degree of polymerization (DP = 15−20). With the same raw materials, Huang et al.[37] conducted the reaction using microwave irradiation and indicated that under the optimum condition (molar ratio of MA/NH_3 = 1.2, power = 900 W, 3.5 min), the yield and M_w were 95% and 1.46 kDa, respectively. Freeman et al.[38] used maleamic acid for PASP synthesis in oven or reactor and the effect of several parameters such as solvent, time, temperature, and processing aid was tested in an effort to improve M_w. However, the highest reported M_w was 2.15 kDa when the reaction was conducted in an oven at 240 °C for 20 min. In addition, maleamic acid can be prepared by reacting maleic anhydride with anhydrous ammonia or by heating the monoammonium salt of maleic acid. Recently, Fukumura et al.[39] reported mixing the monomer with a tertiary amine to convert carboxyl groups of the monomer to tertiary amine salt.

https://doi.org/10.1021/acsbiomaterials.1c00150
ACS Biomater. Sci. Eng. XXXX, XXX, XXX−XXX

Table 1. Summary of Molecular Weight (M_w, M_n, M_v), Mass Dispersity ($Đ_M$), and Yield As a Function of Important Reaction Parameters

no.	T (°C)	time (h)	catalyst (with respect to ASP)	solvent	yield (%)	M_n, M_w, or M_v (kDa)	$Đ_M$	ref
1	200	7	H_3PO_4 (5 wt %)		98	M_w: 19	n.a.	21
2	200	7	H_3PO_4 (10 wt %)		98	M_w: 24	n.a.	
3	200	7	CH_3SO_3H methanesulfonic acid (5 wt %)		99	M_w: 8.8	n.a.	
4	200	7	H2SO4 (5 wt %)		99	M_w: 7.2	n.a.	
5	200	7	*p*-CH3C6H4SO3H (5 wt,%)		99			
6	260	7	none		96	M_w: 9	n.a.	
7	200	7	none		41	M_w: 7.4	n.a.	
8	260	1 kg/h (extruder)	none		16		n.a.	
9	200		H_3PO_4 (10 wt %)		79	M_w: 22	n.a.	
10	260		H_3PO_4 (10 wt %)		99	M_w: 24	n.a.	
11	260	3 kg/h	H_3PO_4 (10 wt %)		99	M_w: 23	n.a.	
12	110−111	4.5	H_3PO_4 (7 wt %)	toluene	0			25
13	164−166			mesitylene	77	M_w: 24.8	1.5	
14	152−153			DMF	0			
15	158−159			sulfolane	89	M_w: 19	1.5	
16	110−111			toluene/sulfolane	0			
17	150−152			mesitylene/DMF	59	M_w: 12.9	1.2	
18	160−162			mesitylene/NMP	96	M_w: 24.5	1.6	
19	176−178			diethylbenzene/sulfolane	96	M_w: 49.3	1.9	
20	160−162			mesitylene/sulfolane	96	M_w: 64.3	1.9	
21	164−166		trichloroacetic acid	mesitylene/sulfolane	0			
22	160−162		*p*-toluenesulfonic acid	mesitylene/sulfolane	89	M_w: 27	1.5	
23	160−162		sulfuric acid	mesitylene/sulfolane (7/3)	96	M_w: 27.9	1.6	
24	260	6		mesitylene/sulfolane (7/3)	>96	M_w: 9		26
25	180	3.5	H_3PO_4 (50 mol %)	mesitylene/sulfolane (7/3)		M_w: 70		
26	reflux	4.5	H_3PO_4 (10 mol %)	mesitylene/sulfolane (7/3)		M_w: 64.3		
27	200	7	H_3PO_4 (10 mol %)	mesitylene/sulfolane (7/3)		M_w: 14		
28	180	7	H_3PO_4 (10 mol %)	mesitylene/sulfolane (7/3)		M_w: 12		
29	200	7	H_3PO_4 (3 mol %)	mesitylene/sulfolane (7/3)		M_w: 9.9		
30	260	16 min (extruder, 30 rpm)	H_3PO_4 (10 mol %)			M_w: 24		
31	260	16 min (extruder, 120 rpm)	H_3PO_4 (10 mol %)			M_w: 23		
32	260	16 min (extruder, 30 rpm)	H_3PO_4 (5 mol %)			M_w: 24		
33	260	6			>97	M_w: 5.2 M_n: 1.8		16
34	n.a	n.a	H_3PO_4 (16 mol %)	mesitylene/sulfolane (ratio n.a.)	n.a	M_v: 7−18.5		27
35	190	6.5	1/1 (w/w ASP/H_3PO_4)		n.a	M_v:33−34		
36	270	8.5			72%	M_w: 4.4 M_n: 3.57	1.23	17
37	240	8	H_3PO_4 (10 wt %)		83.5	M_w: 8.5 M_n: 5.19	1.63	
38	170	10	H_3PO_4 (5 mol %)	sulfolane (200 mL for 40 g of ASP)	85−95	M_w: 17.2 M_n: 22.8	1.32	28
39	180	7	1/1 (w/w ASP/H_3PO_4)		95	M_v: 31.5		29
40	200	6.5	2/1 (w/w ASP/H_3PO_4)			M_n:15.7 M_v: 44.9	2.86	30

This enabled them both to conduct the reaction at low temperature (90−130 °C) and to obtain molecular weight of around 10 kDa.

Overall, despite yielding low-M_w PASP, this method is still utilized in industry for antiscalant applications due to the inexpensiveness of the raw materials (MA and NH_3).[34,40] The reason for achieving low molecular weight could possibly be attributed to the difficulties associated with bulk polymerization (i.e., high viscosity and inefficient heat transfer and mixing). Despite little investigation, the molecular weight may be improved by manipulation of the reaction parameters. For example, the polymerization step can be conducted in only H_3PO_4 or sulfolane/H_3PO_4 which were effective in increasing the M_w.[25,29]

2.3. Synthesis of Block Copolymers of ASP. Due to its biodegradability, PASP has been coupled with other synthetic degradable polymers such as poly(ethylene glycol) (PEG) and poly(lactic acid) in the form of block,[41] random,[42] and graft[27] copolymers. Such copolymers can be used to generate micellar nanostructures, which are widely utilized as biodegradable

https://doi.org/10.1021/acsbiomaterials.1c00150
ACS Biomater. Sci. Eng. XXXX, XXX, XXX−XXX

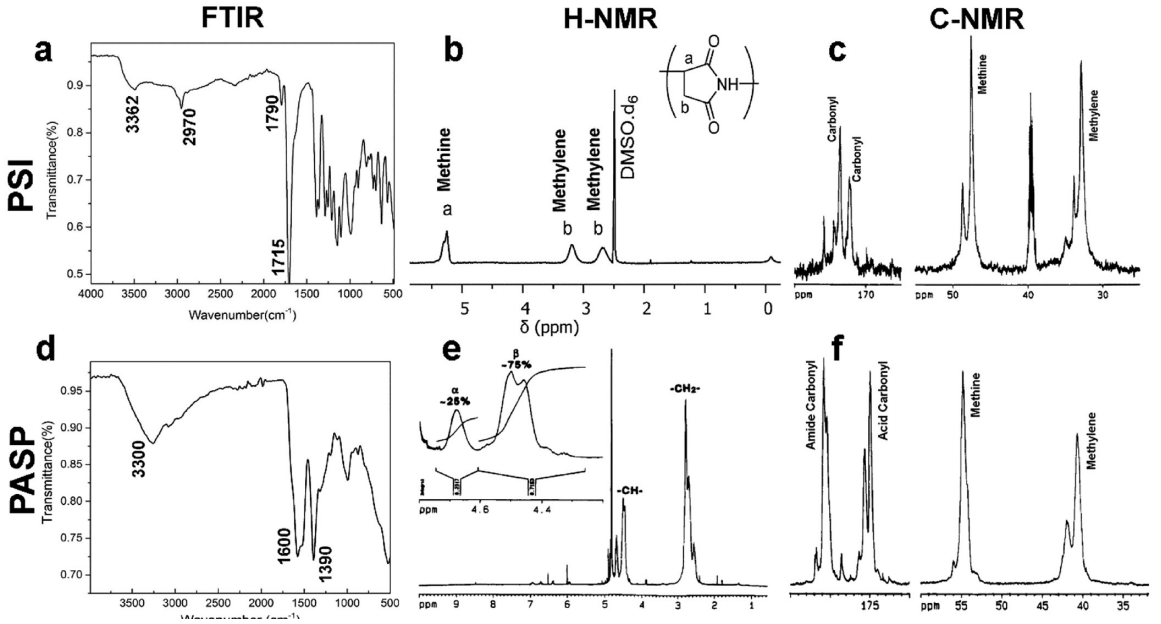

Figure 2. Chemical characterization of PSI and PASP. (a, d) FTIR, (b, e) ^{1}H NMR, and (c, f) ^{13}C NMR of (a–c) PSI and (d–f) PASP. The inset in e shows the magnification of 4.2–4.8 ppm for methine region. (a, d) Reproduced with permission from ref 5. Copyright 2014 Elsevier. (b) Reproduced with permission from ref 63. Copyright 2016 Elsevier. (b, c, e, f) Reproduced with permission from ref 17. Copyright 2014 American Chemical Society.

delivery vehicles.[43] Block copolymers that have a PASP block can be synthesized using N-carboxyanhydrides (NCA) such as β-benzyl-L-aspartate (BLA) NCA, which is initiated by an amine, such as PEG amine to form Benzyl-PASP-*block*-PEG. The polymerization of BLA-NCA not only decreases chain branching and chirality but also yields narrow molecular weight distribution ($Đ_M$ of close to 1; $Đ_M = M_w/M_n$).[44] Additionally, this reaction occurs at room temperature and releases carbon dioxide as the byproduct. Benzyl protection can be removed either by alkaline hydrolysis or acid treatment to yield PASP.[41,44−47]

In a typical reaction, as shown in Figure 1b, ASP (1) is first protected with benzyl group to yield b-benzyl-L-aspartate (BLA) (2). BLA is then converted into BLA-NCA (3) by condensation with phosgene. Reaction with α-methyl-ω-aminopolyoxyethylene (m-PEG-NH_2) gives the block copolymer (PEG-benzyl PASP) (4). After purification, the protective benzyl groups are removed by alkaline hydrolysis to obtain PASP-*b*-PEG (5).[46] It should be noted that the polymerization of BLA-NCA occurs from terminal amino groups of m-PEG-NH_2 (room temperature, 16−24 h), and instead of PEG, other macroinitiators with NH_2 end groups can be utilized as well.[41]

Another way for synthesis of block copolymers is the reaction of PSI with macroinitiators having succinimidyl succinate end groups (Figure 1c). The latter reacts with the NH_2 groups at the end of PSI homopolymer chains through a nucleophilic ring-opening reaction.[48,49] For example, for preparation of PEG-*b*-PSI, mPEG-succinimidyl succinate was reacted with PSI in DMF at 40 °C for 48 h. Diverse morphologies of the cross-linked micelles were fabricated by varying the cross-linker/succinimide ratio.[49]

Random copolymerization of aspartic acid with different monomers such as lactic acid, citric acid, and malic acid has also been reported in the literature.[13,42,50−54] For example, Han et al.[50,51] conducted copolymerization of aspartic acid and lactic acid under nitrogen flow at 180 °C for 6 h followed by a further reaction at 160 °C for 20 h. Tudorachi et al.[42] synthesized the same copolymers through solution polycondensation of oligomers of lactic acid and ASP in DMF/toluene. Other protocols for preparation of such copolymers have been proposed as well.[52,53] Such random copolymers could be highly advantageous for biomedical applications as lactic acid can increase hydrophobicity while maintaining the biodegradability and biocompatibility features.[55]

3. CHARACTERIZATION

This section of the review focuses on typical characterization methods used for PSI and PASP in terms of chemical structure which are usually carried out by Fourier-transform infrared spectroscopy (FTIR), carbon-13 and hydrogen nuclear magnetic resonance (^{13}C NMR and ^{1}H NMR, respectively).

3.1. FTIR. PSI and PASP have been studied using FTIR by several researchers.[56−62] The FTIR spectra of PSI and PASP are shown in Figure 2a, d, respectively. The characteristic peaks of PSI are seen at wavenumbers at 1795 (weak), 1713 (sharp), 1390 (sharp), 1361 (sharp), and 3362 cm^{-1} (broad). The absorption bands at 1713 and 1795 cm^{-1} were attributed to the coupled effect of two neighboring carbonyl groups in the succinimide. Hydrolysis of the succinimide results in disappearance of these peaks after ring-opening.[59] For PASP however, the characteristic peaks are usually observed at wavenumbers at 3280 (broad), 1560 (sharp and relatively broad), 1390 (sharp), 1620 cm^{-1} (shoulder).[61,62] It should be noted that possibly because of different degrees of neutralization, the presence of counterion, and different position of carboxylic acid group (i.e., α or β) in PASP, the characteristic peaks of PASP in the literature differ to some extent; however, the overall pattern is similar.[57−59,61,62]

3.2. ^{1}H NMR. Regarding H NMR of PSI in d_6-DMSO, the characteristic peaks are at 2.69, 3.21, and 5.26 ppm.[17] The first two peaks with approximately similar intensity are related to methylene protons, while the last one is attributed to methine

https://doi.org/10.1021/acsbiomaterials.1c00150
ACS Biomater. Sci. Eng. XXXX, XXX, XXX−XXX

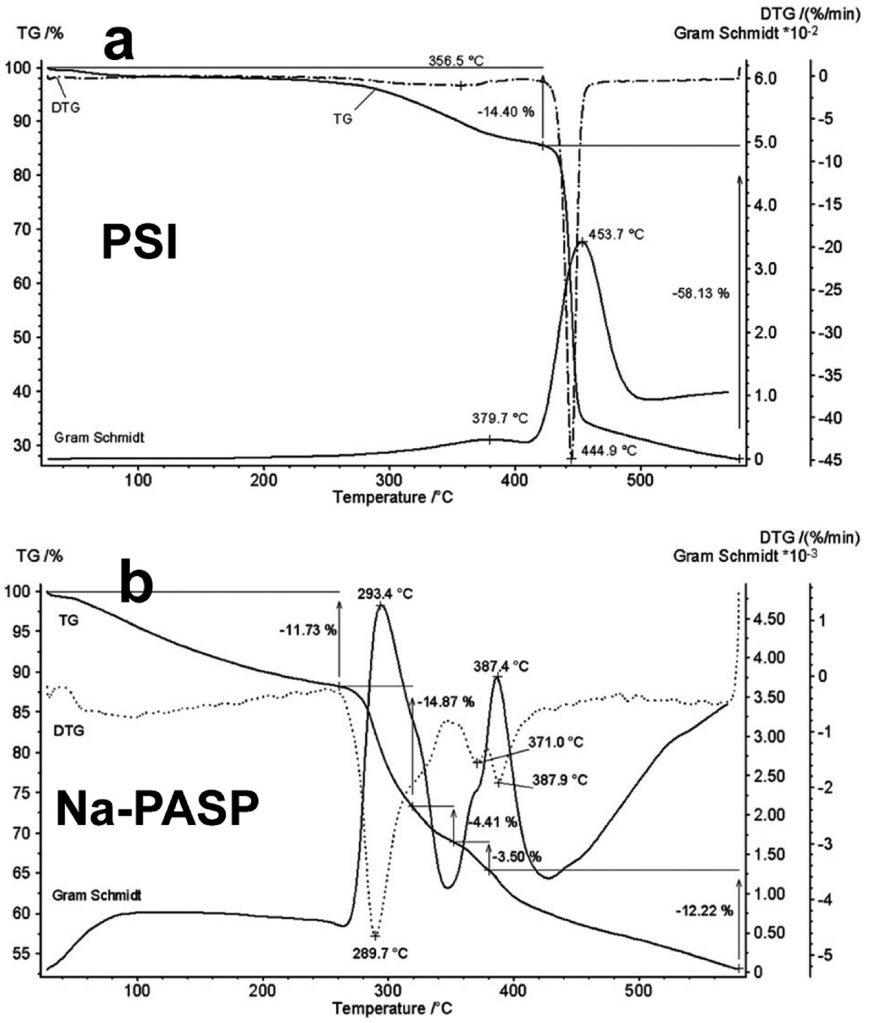

Figure 3. Thermal properties of PSI and PASP. TGA and DTG curves of (a) PSI and (b) PASP. Reproduced with permission from ref 64. Copyright 2011 Elsevier.

protons (Figure 2b). For PASP in D_2O, the methine proton is observed at around 4.7 and 4.5 ppm, while the methylene proton is seen at 2.8, 2.7, and 2.55 ppm. The peaks at 4.7 and 4.5 ppm are attributed to α- and β-PASP, respectively, as shown in the inset (Figure 2-e).[17] It should also be noted that protons of acid or amide are not observed as they are exchanged with D_2O in a neutral medium of pD = 7.4.

3.3. ^{13}C NMR. Regarding the ^{13}C NMR of PSI, because the two carbonyl groups of PSI are inequivalent, two distinct peaks are observed at 173 and 174 ppm. The peaks at 47 and 32 ppm are attributed to carbons of methines and methylenes, respectively (Figure 2c).[17] For the ^{13}C NMR of PASP, carbons of amide and acid carbonyl are seen in the range of 170−185 ppm with two distinct resonances (downfield for acid and upfield for amide). The carbons of methine and methylene have resonances at 51−57 and 37−44 ppm, respectively (Figure 2f). The other small resonances were ascribed to the end groups and structural variations.

3.4. Other characteristics. The thermal stability of PSI and PASP was studied by Tudorachi et al.[64] who found that PSI has a two-step degradation and is more thermally stable than PASP especially at temperatures lower than 300 °C (Figure 3). The temperatures at which 10% weight loss occur for PSI and Na-PASP (sodium salt of PASP) are 375 and 199 °C, respectively. The final weight loss values at 600 °C for PSI and PASP were respectively found to be 72 and 46%, suggesting higher stability of PASP at high temperatures. This could be attributed to the formation of ionic clusters in PASP due to the presence of sodium ions that undergo self-association to form ionic aggregates.[24] Subsequently, these regions hinder chain mobility and increase glass transition and thermal stability. Although interpretation of different stages of the weight was stated to be complex, elimination of adsorbed water as well as other volatile compounds and C−C linkage scission were found to occur in the early and last stages, respectively.

Determination of PASP concentration particularly when it is employed as an antiscalant for water purification is of great importance. Titration can be adopted because PASP is a polyacid polyelectrolyte.[65] Fluorometry has also been found to provide precise results in the case of PASP and its salts.[66] In this technique, the solution is excited and the intensity of the emitted fluorescent light is measured as a function of the excitation and emission wavelengths. The excitation and emission wavelengths of PASP are at 336 and 411 nm, respectively and so the concentration of PASP and its salts can be detected by plotting a standard curve.

https://doi.org/10.1021/acsbiomaterials.1c00150
ACS Biomater. Sci. Eng. XXXX, XXX, XXX−XXX

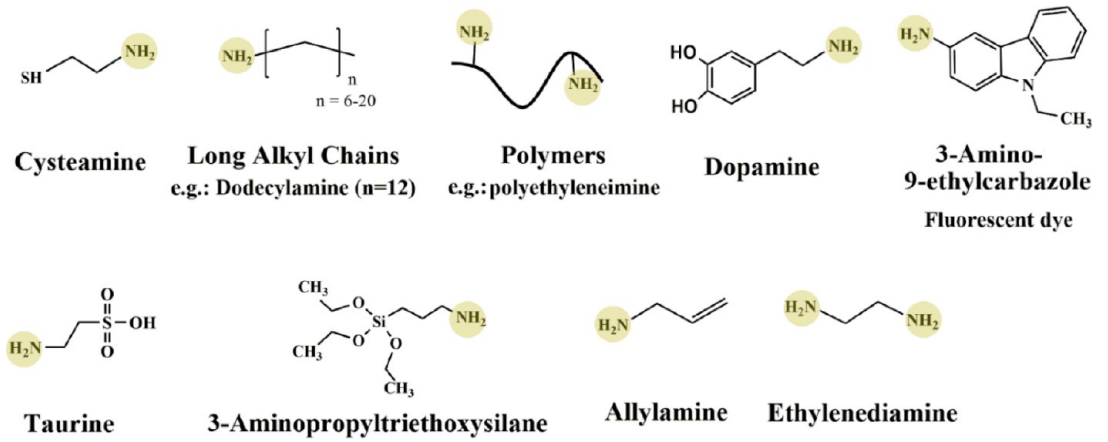

Figure 4. Some examples of molecules bearing primary amine groups for PASP and PSI modification. The NH_2 group will react with succinimide units of PSI, yielding an amide bond (CONH-R). The -R- functionality could be a wide variety of molecules ranging from silanol to thiol.

4. MODIFICATION

Chemical structure of PASP can be customized by introducing different functional groups for diverse applications. This is generally carried out via ring-opening reaction of PSI because it reacts readily with primary amines (i.e., NH_2 functionality) under mild conditions even in the absence of a catalyst.[67] The PSI backbone via such reaction can be functionalized with a wide variety of species ranging from polymers to long alkyl chains as shown in Figure 4. Employing molecules bearing two or more amine groups enables the fabrication of cross-linked PSI, and subsequently PASP-based hydrogels.[68,69] The hydrogels can also be further modified to be responsive to other stimuli such as temperature and redox state. In the following subsections, PASP modifications including grafting of thiols, dopamine, polymers, an alkyl chains are discussed. However, PASP modification is not limited to such cases, and a much wider range of agents such as fluorescent dyes,[15] cyclodextrin,[70] sulfonic acid,[71] zwitterions,[72] and silanol[73] groups can be applied as well.

4.1. Thiols. One of the most common types of functionalization is PASP thiolation using thiol-containing molecules (−SH) such as cysteamine (CYS).[29,74−80] Thiol groups can react with each other under oxidizing conditions, forming disulfide bonds (−S−S−) and thus giving rise to cross-linked PASP (i.e., hydrogel).[68] This feature can open up wide avenues for developing injectable PASP-based hydrogels. For example, Szilagyi et al.[29] incorporated high levels of thiols (30 mol %) into PASP and showed that oxidation leads to fast in situ gelation (ca. 71 s) as well as a high storage modulus (16 kPa) (as shown in Figure 5a).

More interestingly, the reaction is reversible, which allows one to tune the degree of cross-linking by changing the concentration of the reducing or oxidizing agents, while maintaining network integrity when a permanent cross-linker is also used.[22,80,81] In other words, redox-responsive hydrogels can be developed through simultaneous thiolation and use of a permanent cross-linker. For example, Gyarmati et al.[80] demonstrated reversible swelling/deswelling behavior of the thiolated PASP hydrogels under oxidizing/reducing states (as shown in Figure 5b). In another study, nanogels were prepared with both permanent and cleavable redox-sensitive cross-linker as seen in Figure 5c. Apart from reducing agents, high pH values can also break and dissociate the disulfide bonds.[22] Thiolation also improves adhesion to the mucus membrane of the body and thus is suitable for bioadhesion in drug delivery, which will be discussed in section 7.4.[82−84]

4.2. Long Alkyl Chain. The other type of modification focuses on reducing PASP hydrophilicity by incorporation of long alkyl chains. Because of the self-association of lipophilic chains, such modification allows preparation of the PASP-based particles and/or micelles in water which improves dissolution and loading capacity of hydrophobic drugs. For instance, octadecyl amine as well as dopamine was grafted onto PASP for increasing hydrophobicity, encapsulation of hydrophobic drugs (e.g., curcumin), and subsequently the formation of PASP-based particles for drug delivery (shown in Figure 5d).[85]

Incorporation of long alkyl chains can also lead to surface-active properties and a new generation of degradable surfactants.[28] The surfactant properties can be adjusted depending upon the degree of substitution and the length of alkyl chain. Kang et al.[28] comprehensively investigated the self-aggregation of modified PASP in water as a function of the degree of substitution, the length, and the backbone stiffness of grafted chain. They found that dodecyl- (C12) and hexadecyl (C16)-grafted PASP show surface-active properties, which can be exploited as emulsifying agents. In contrast, grafting with octadecyl (C18) exhibited abnormal behavior because of lower flexibility, as it is under solid state at room temperature. As can be seen in Figure 5e, PASPs modified with C12 and C16 (DS of 10%) exhibit the conventional trend of surfactant surface tension as a function of concentration (i.e., exponential decrement).

As such, the addition of dodecyl (C12)-PASP to manganese-(IV) oxide nanoparticles (MONPs) dispersed in water exhibited a significant improvement in terms of dispersibility and stability.[86] In another study, hydrophobic MONPs were successfully dispersed in water employing PASP and were utilized for magnetic resonance imaging (MRI) of the liver.[87] Comparison of PASP and phospholipid-PEG in terms of stability and r_1 relaxivity revealed the superiority of PASP and its effect on enhancement of T_1 contrast of the MONPs. This was attributed to the more hydrophilic nature of PASP that leads to a better manganese-water interaction. Yang et al.[88] also demonstrated enhanced loading of hydrophobic iron oxide nanocrystals by the addition of octadecyl (C18)-PASP, which further proves stabilization properties of these polymers.

https://doi.org/10.1021/acsbiomaterials.1c00150
ACS Biomater. Sci. Eng. XXXX, XXX, XXX−XXX

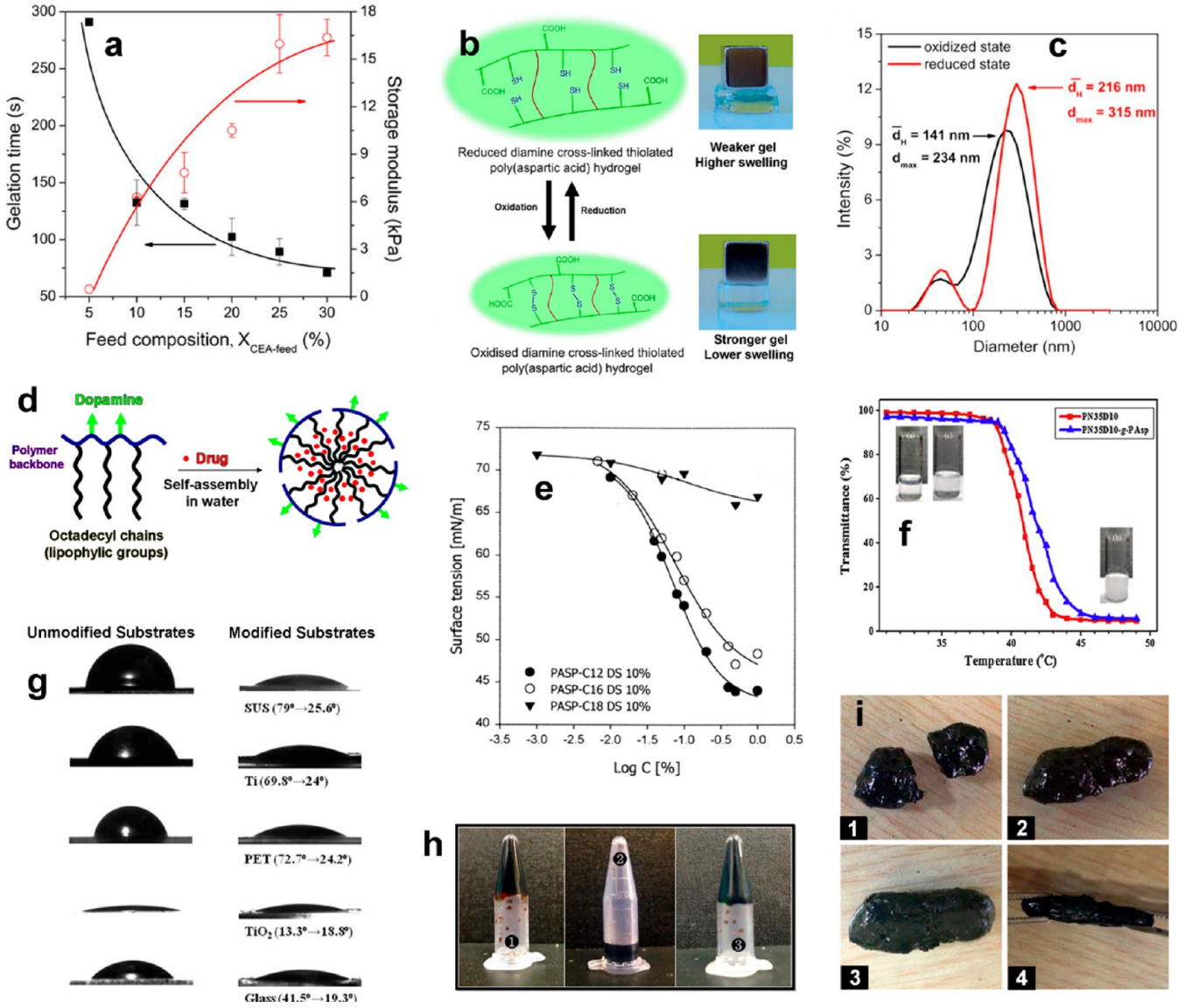

Figure 5. Modification and properties of the resulting PASP. (a) Gelation time and storage modulus of thiolated PASP hydrogels as a function of thiol content (polymer concentration = 10 wt %, in PBS at pH 7.4, T = 25 °C). Reproduced with permission from ref 29. Copyright 2017 John Wiley and Sons. (b) Schematic representation (left panel) of reversible changes of the thiolated PASP hydrogels in response to reduction/oxidation. Photographs (right panel) of PASP hydrogels under a load of 15g in reduced and oxidized states. Reproduced with permission from ref 80. Copyright 2014 Royal Society of Chemistry. (c) Size distribution of thiolated PASP nanogels with permanent cross-linker and cleavable disulfide under reduced and oxidized states. Reproduced with permission from ref 81. Copyright 2018 Elsevier. (d) Schematic representation of long alkyl chain grafting onto PASP chain, subsequent polymer self-assembly and drug loading in water. Reproduced with permission from ref 85. Copyright 2015 Royal Society of Chemistry. (e) Surface tension as a function of concentration of PASP modified with alkyl chains with lengths of 12, 16, and 18 carbons. Reproduced with permission from ref 28. Copyright 2001 American Chemical Society. (f) LCST behavior of PASP modified with poly(*N*-isopropylacrylamide-*co*-N,N-dimethylacrylamide). Reproduced with permission from ref 91. Copyright 2013 Elsevier. (g) Contact angle of different substrates coated with and without dopamine-modified PASP. SUS, Ti, PET, and TiO2 respectively stand for steel use stainless, titanium foil, poly(ethylene terephthalate) (PET), and titanium oxide. Reproduced with permission from ref 103. Copyright 2011 John Wiley and Sons. (h) Photographs illustrating the reversible gel formation of dopamine-grafted PASP/graphene oxide as a result of boron/catechol coordinative complexation. Gelation occurred at pH 9 (1) became solution upon pH reduction to 5 (2), and became gel again by increasing the pH to 9 (3). Reproduced with permission from ref 102. Copyright 2016 Elsevier. (i) Photographs of the corresponding samples (1) cut into two pieces, (2) rejoined pieces, (3) healed sample, and (4) the extension of healed sample. Reproduced with permission from ref 102 Copyright 2016 Elsevier.

4.3. Polymer/Oligomer. Polymers and oligomers have been grafted onto PASP for different purposes such as delivery of bioactive agents and hydrogel preparation. For example, oligoethylenimine was conjugated to PASP for gene delivery because of its positive electrical charge which will be discussed in section 7.4.[89,90] Yeh et al.[91] grafted amine-terminated poly(*N*-isopropylacrylamide-*co*-N,N-dimethylacrylamide) onto PASP to endow the micelles with temperature responsiveness. The micelles exhibited tunable lower critical solubility temperatures (LCST) ranging from 37 to 46 °C by varying the degree of grafting (Figure 5f). Modification of delivery vehicles with PEG is a critical step in reducing immunogenicity by improving their hydrophilicity, thereby prolonging the circulatory time and reducing renal clearance.[92] Hence, the

https://doi.org/10.1021/acsbiomaterials.1c00150
ACS Biomater. Sci. Eng. XXXX, XXX, XXX−XXX

conjugates of PASP with PEG could be promising candidates for delivery systems. However, neither PASP alone nor PASP−PEG conjugates can form micelle/particle in water due to their hydrophilicity, and thus incorporation of another agent such as cholic acid[93] or lauryl amine[27] is necessary. Complex formation through charge neutralization of PASP with a cationic emulsifier (e.g., cetyltrimethylammonium bromide) can also result in stable micelles in water.[94] PASP−PEG nanogels can be fabricated through the hydrolysis of cross-linked PSI−PEG particles which form in aqueous media due to the hydrophobicity of PSI. Park et al.[78] prepared PASP-*g*-PEG nanogels (D < 100 nm) through self-association of PSI−PEG in water (i.e., micelle formation), followed by diamine cross-linking and alkali hydrolysis.

4.4. Dopamine. Catechol (benzenediol) moieties in dopamine exhibit a multifunctional characteristic for the design of mussel-inspired adhesive coatings as it strongly attaches to virtually any substrate and is a well-known agent for surface modification.[95] For instance, An et al.[96] treated a wide variety of surfaces with dopamine-modified PASP. The result was that catechol establishes a strong adhesive bond to synthetic polymers, metals, metal oxides, and ceramics. Such a coating significantly improves surface hydrophilicity as shown in Figure 5g.

Complex formation of catechols with boron and iron ions can also be tailored for the design of state-of-the-art soft materials such as responsive hydrogels or self-healing materials.[97−99] Gong et al.[100] found that the complexation of ferrous ions (Fe^{3+}) with dopamine-modified PASP leads to excellent photothermal properties when irradiated with near-infrared (NIR) lasers. Using dopamine:Fe^{3+} molar ratios of 3:1, the most marked photothermal effect was observed where a temperature increase of 27 °C was achieved (5 min at 808 nm). Additionally, the polymer/Fe^{3+} interaction can form spherical nanostructures with an average size of 116 nm. Complexation with Fe^{3+} ions was also exploited for the preparation of injectable PASP hydrogels modified with dopamine (gelation time around 1 min).[100] It was suggested that the resulting cross-linking points are composed of both Fe^{3+} coordination as well as covalent quinone−quinone bonds. Utilizing the same coordination concept for gelation, Wang et al.[101] prepared PASP-based aerogels reinforced with reduced graphene oxide (rGO). The same group also showed that cross-linking with boric acid results in reversible hydrogels through pH change with autonomous self-healing ability as a result of boron−catechol coordination as shown in Figure 5h, i.[102]

5. DEGRADATION

PASP is a polypeptide and so it can be degraded under physiological or biological conditions.[104−106] Because of the susceptibility of amide linkages in the backbone to hydrolysis, PASP modification may change the degradation rate but does not prevent it.[104] Several degradation agents and conditions have been examined and are summarized in Table 2. Nakato et al.[105] found that the biodegradability of PASP is not affected by the type of amide linkage (α or β) or ASP chirality. Alford et al.[106] showed that PASP is degraded in activated sludge. Around 95% of PASP degradation was achieved after 23 days with the most degradation occurring in less than 5 days. Tabata et al.[107] studied PASP microbial degradation in river water at 25 °C and showed that PASP with a molecular weight of 20 kDa undergoes complete degradation after 15 days (Figure

Table 2. Degradation of PASP under Different Conditions[a]

degradation agent	free polymer or gel; cross-linker	degradation site	degradation time (day)	results	ref
activated sludge	free PASP	n.d.	28	degradability is not affected by the type of amide linkage (α or β) or ASP chirality	105
activated sludge	free PASP	n.d.	28 and 23 days for low- and high-biomass sludge, respectively	PASP is degraded in activated sludge; majority of degradation occurs in the first 5 days	106
natural river water	free PASP	n.d.	15	strain KP-2 and *Sphingomonas* sp. KT-1 isolated bacteria from river water were responsible for degradation of high and low M_w PASP, respectively	107
river water	free PASP	β-amide linkage	n.d.	Ddegrading enzyme from *Sphingomonas* sp. KT-1 selectively degrades the β-amide linkage connecting with β- units	108
water taken from a sewage river	free copolymer of poly(ASP-lysine)	n.d.	after 28 days, 80% degradation occurs (50% lysine)	higher lysine content or lower M_w increased degradation rate; Cu^{2+} complexation with the copolymer lowered degradation rate	109
α-chymotrypsin	hdrogel; 1, 6-hexamethylene diamine	n.d.	n.d.	2 wt % α-chymotrypsin after 54 days led to ca. 80% hydrogel degradation	110
α-chymotrypsin	hydrogel; 1, 6-hexamethylene diamine	n.d.	ca. 4 days	α-chymotrypsin induces through bulk-erosion process; degradation process initiates from cross-linking points followed by amide bonds cleavage, and consequently disintegration of the hydrogel	111
trypsin	hydrogel; ethylenediamine	n.d.	7 days in 0.05 mg/mL trypsin/PBS solution	trypsin led to 83 wt % weight loss of hydrogel nanofibers after 7 days	112
trypsin, dispase and collagenase I	hydrogel with 1,4 diaminobutane (DAB) and CYS	disulfide bonds of the gel junctions	n.d.	collagenase I was stronger degradation agent	113,115

[a]"n.d." stands for not determined.

https://doi.org/10.1021/acsbiomaterials.1c00150
ACS Biomater. Sci. Eng. XXXX, XXX, XXX−XXX

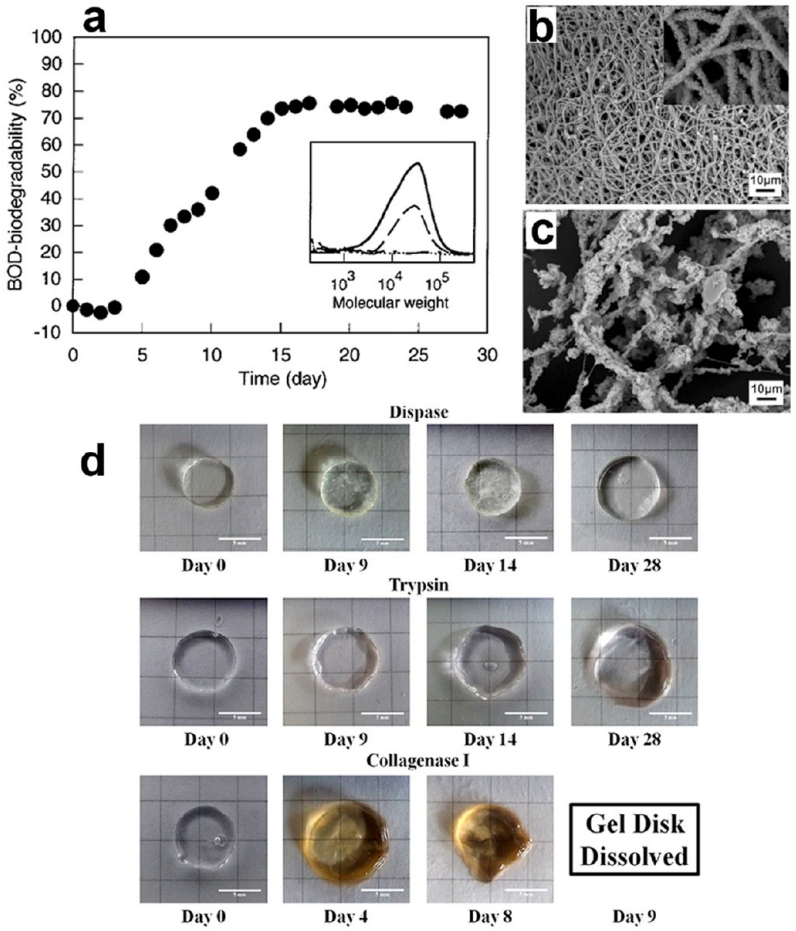

Figure 6. Biodegradation of PASP under different conditions. (a) Biodegradation curve of PASP in fresh river water at 25 °C. Inset shows time-dependent M_w changes of PASP in fresh river water. Reproduced with permission from ref 107. Copyright 2000 American Chemical Society. (b, c) SEM photographs of PASP hydrogel upon biodegradation in trypsin/PBS solution: (b) 1 day and (c) 4 days. Reproduced with permission from ref 112. Copyright 2017 Springer Nature. (d) Degradation of PASP-CYS hydrogel disks in the presence of trypsin-ethylenediaminetetraacetic acid (EDTA), dispase, and collagenase I. Reproduced with permission from ref 113. Copyright 2016 American Chemical Society.

6a). They isolated a bacterium (strain KP-2) that is a member of *Pedobacter* and *Sphingomonas* sp. KT-1 from river water. The *Pedobacter* degraded high-molecular-weight PASP ranging from 5 to 150 kDa. In contrast, *Sphingomonas* sp. KT-1 degraded only low-M_w PASP below 5 kDa. It was concluded that the mixture of the two isolates is needed for complete degradation. In another study, the same group[108] found that PASP-degrading enzymes fall in the category of serine hydrolases. The analysis of chemical structure of the degraded products revealed that the purified enzyme selectively degrades the β-amide linkage connecting with β-ASP units.

Yu-ling et al.[109] investigated the biodegradability of poly(ASP-lysine) copolymers by carbon dioxide evolution tests. The degradation after 10 and 28 days was respectively 35 and 80%. Higher lysine content in the copolymer or lower molecular weight accelerated degradation. The effect of α-chymotrypsin (0.4 and 2 wt %) as a digestive enzyme on PASP hydrogel degradation was also examined at pH 7.5.[110] Weight loss of around 90% was obtained after 54 days with 2 wt % of the enzyme. Yang et al.[111] proposed that α-chymotrypsin induces degradation through the bulk-erosion process. The results in terms of viscosity, molecular weight, and swelling suggested that the degradation process initiates from cross-linking points followed by amide bonds cleavage and consequently disintegration of the hydrogel. The effect of trypsin, a serine protease, on the degradation of Na-PASP hydrogel nanofibers was also evaluated.[112] The addition of 50 ppm of trypsin led to 83 wt % weight loss after 7 days. The SEM micrographs demonstrated a significant change in morphology of the nanofibers during biodegradation. (Figure 6b, c). Juriga et al.[113] investigated the degradation of PASP hydrogels in different enzyme solutions (trypsin, Dispase, and collagenase I) (Figure 6d). When PBS buffer was used as a negative control, degradation was not observed up to 42 days. The enzyme effectivity for degradation was found in the following order: collagenase I (0.3 wt %) > trypsin (0.05 wt %) > Dispase (0.4 wt %). As seen in Figure 6d, the gel disk completely dissolves in the presence of collagenase I after 9 days. The in vitro degradation of copolymers of ASP and L-glutamic acid by papain in a pseudoextracellular fluid solution (p 4.75 and 7.4, T = 37 °C) showed that the degradation occurs by random-chain scission.[114] Although PASP has been widely employed in biomedical applications, there have been no in vivo degradation studies of PASP reported so far.

https://doi.org/10.1021/acsbiomaterials.1c00150
ACS Biomater. Sci. Eng. XXXX, XXX, XXX−XXX

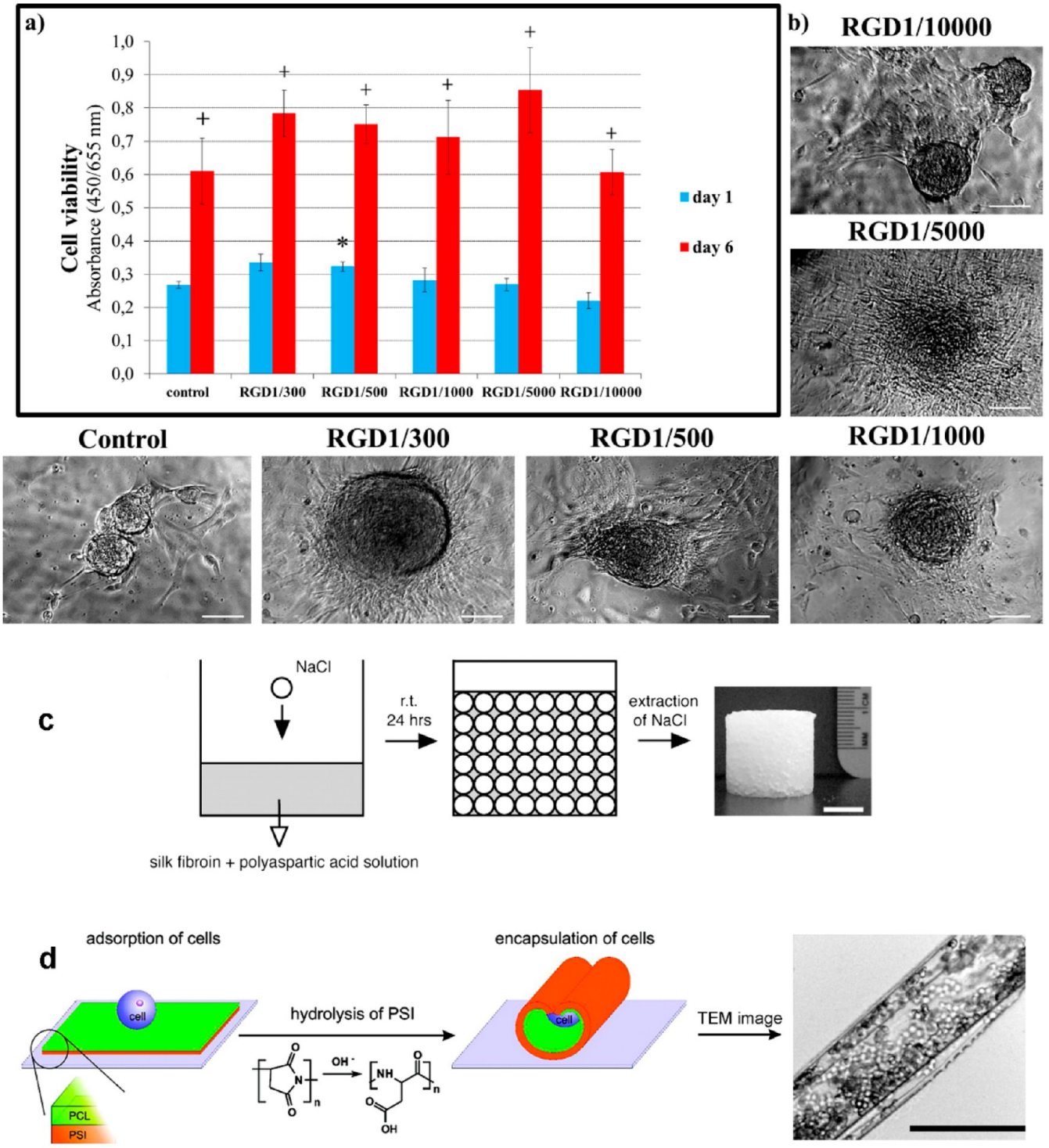

Figure 7. The use of PASP for cell proliferation and cell encapsulation. (a) Cell viability of MG-63 after 1 and 6 days, (b) cell morphology on hydrogel scaffolds with various amounts of RGD. Data are presented as arithmetic mean ± standard error of the mean. *p < 0.05 compared to control. + p < 0.05 compared to day 1. The scale bars are 100 μm. Reproduced with permission from ref 113. Copyright 2016 American Chemical Society. (c) Schematic representation of the formation of porous composite scaffolds. Reproduced with permission from ref 118. Copyright 2008 Elsevier. (d) Schematic representation of self-rolling of the PSI/PCL bilayer films to tubes, leading to encapsulation of the yeast cells as seen in the microscopic image with the scale bar of 100 μm. Reproduced with permission from ref 30. Copyright 2011 American Chemical Society.

6. BIOCOMPATIBILITY OF PASP AND ITS DERIVATIVES

Biocompatibility of PASP and its derivatives (i.e., usually polyaspartimides) have been indicated in various studies and attributed to their protein-like backbone structure.[116−118] In vitro studies showed PASP nontoxicity to 3T3 fibroblasts as well as PC-3 cells (prostate cancer cell) with IC_{50} > 3 mg/mL.[116] PASP-based hydrogels were efficiently utilized as scaffolds for cultivation of osteoblasts (MG-63), further verifying PASP biocompatibility.[113] Oral administration of

https://doi.org/10.1021/acsbiomaterials.1c00150
ACS Biomater. Sci. Eng. XXXX, XXX, XXX−XXX

PASP/iron−zinc microrockets to mice was performed for delivery of DOX.[119] The device is propelled by the acidic condition of the stomach due to the reaction of zinc with acid, releasing hydrogen gas. No observable side effect such as hunched posture, pain, or lethargy was noticed (6 days monitoring). Histological analysis of the stomachs also showed no difference in the length and numbers of crypt and villi and no gastric inflammation was noticed when compared to water-treated group. PASP was chosen to coat iron oxide nanoparticles to reduce toxicity. Blood cytometry of the mice (time and dose dependent) revealed biocompatibility of the particles, although comparison was not made between uncoated and coated particles.[120] Juriga et al.[121] called the PASP hydrogels "fully amino acid−based gels" and verified a high viability level of human periodontal ligament-derived cells on the gels as scaffold. A recent study has also verified in vitro and in vivo biocompatibility of PASP-based hydrogels loaded with copper peptide GHK-Cu for wound-healing purposes.[122]

Furthermore, chemical modification of PASP should not adversely affect the biocompatibility unless the attached agent is degraded, released and pose toxicity. For example, grafting high amount of L-histidine and L-lysine did not result in toxicity to 3T3 cells for 24 h incubation.[123] The polymer obtained by complete conversion of succinimide units by octadecylamine (C18) and dopamine did not show significant toxicity to 293T cell line (studied concentration range 0−100 μg/mL). The polymer was used as bioadhesive for wound healing applications.[124]

7. BIOMEDICAL APPLICATIONS OF PASP AND ITS DERIVATIVES

Because of their biodegradability, and biocompatibility, PASP-based materials could be regarded as promising candidates to be utilized in diverse areas of biomedical applications.[6] Ease of chemical modification could also facilitate covalent attachment of not only PEG for prolonging circulation time but also peptides and antibodies for targeted delivery.[125,126] In light of the above-mentioned, this part of the review focuses on the application of PASP as a biomaterial.

7.1. Scaffold. Scaffolds are mainly employed for the cultivation of cells that are derived from damaged tissue for the purpose of regeneration.[127,128] To be employed as a scaffold, a suitable material should be biocompatible, biodegradable, mechanically strong, and porous. Additionally, cells should be able to function normally on the scaffold. As another important criterion, inflammation or scaffold rejection by the body should not occur after implantation. Finally, the scaffold should spontaneously degrade into nontoxic products and be able to be gradually cleared without intervention.[129,130] PASP has been shown to meet these requirements and thus may be regarded as a potential candidate for tissue engineering as discussed below.

Juriga et al.[113] cultivated osteoblasts (MG-63) on PASP hydrogels with or without RGD. They also conjugated thiol (S−H) groups to PASP and found that thiolation greatly contributes to the adhesion, survival and proliferation of the cells. This was attributed to the affinity of mammalian cells to thiol groups. The adhesion and proliferation was found to be independent of RGD content (Figure 7a). Additionally, the presence of RGD induced the formation of compact clusters of cells (Figure 7b). However, in another study, the introduction of RGD to PASP and its subsequent use as a component of the scaffold enhanced fibroblast (3T3 cell line) adhesion.[131] This can be attributed to RGD receptors on the surface of mammalian cells.[132] An et al.[103] treated various substrates including glass, SUS, Ti, PET, and TiO_2 with PASP-based polymers and showed that fibroblast (L929 cell line) proliferation is highly stimulated by such a coating. Flat and nonporous surfaces have the least surface area and are not generally effective for cell proliferation. Development of nanofibers can potentially create a highly porous structure, which is useful for nutrient distribution for cell growth.[74,133] Scaffolds based on nanofibers of thiolated PASP hydrogels were fabricated through reactive electrospinning and was suggested as a potential material for use as an artificial extracellular matrix.[134] In another study, porosity was induced into PASP/silk fibroin composite scaffolds using a high volume fraction of NaCl crystals (4 g of NaCl for 2 mL of solution) (schematically shown in Figure 7c).[118] Due to supersaturation, the salt was insoluble and remained in the physical form of crystals. After scaffold formation, the salt was extracted from the scaffold, leading to the formation of a porous structure. The scaffolds were then premineralized with CaP and subsequently seeded with human bone marrow stem cells (hMSC). Increasing the PASP content enhanced apatite deposition which was attributed to the high affinity of ASP groups to CaP and apatite crystallites. However, higher apatite deposition was accompanied by less uniform cell distribution due to the hindrance of cell migration, which necessitates precise control over the PASP/apatite ratio.[118]

Shape-changing polymers have also been recently used as scaffolds to enable patterning and encapsulation of cells.[30,135] For example, PASP/polycaprolactone (PCL) tubes were fabricated through rolling of PSI/PCL thin films and employed to encapsulate yeast cells (shown in Figure 7d).[30] Self-rolling behavior originated from slow PSI to PASP conversion upon hydrolysis in phosphate buffer solution (PBS) pH 7.4. The subsequent swelling of PASP (as the bottom layer) produces internal stresses in the bilayer films, which leads to the self-rolling process, resulting in encapsulation of the cells. The internal stress is created because PCL does not swell, but the dimensions of PSI increases upon swelling.

7.2. Surface Coating. Surface modification of biomaterials ranging from devices to particles is a crucial step to prevent biofouling. Biofouling is defined as spontaneous protein adsorption and bacterial colonization of surfaces.[136] Improving surface hydrophilicity via the introduction of PEG and zwitterions can significantly reduce biofouling and nonspecific protein absorption.[98] In contrast to PEG which is a nonionic polymer, the zwitterions bear both negative and positive charges, which yields neutral net charge.[99] Modification of PSI by either L-histidine or L-lysine led to zwitterionic-based PASP.[72] Surface coating of silicon wafers by the modified PASPs was shown to decrease the water contact angle from 54 to 35 and 19°, respectively. As a consequence, the protein adsorption significantly decreased, which was consistent with the contact angle results. In another study, zwitterionic PASP was synthesized with L-histidine methyl ester.[137] The introduced imidazole groups and the remaining pendant acid groups of PASP served as cationic and anionic functional groups of the polymer, respectively. Coating of silicon wafers with the polymer effectively prevented the adsorption of fibrinogen. Xu et al.[138] also demonstrated that partial modification of PSI with tetraethylenepentamine results in zwitterionic PASP core−shell particles through self-assembly (size 80−300 nm). Protein adsorption of the polymer was

https://doi.org/10.1021/acsbiomaterials.1c00150
ACS Biomater. Sci. Eng. XXXX, XXX, XXX−XXX

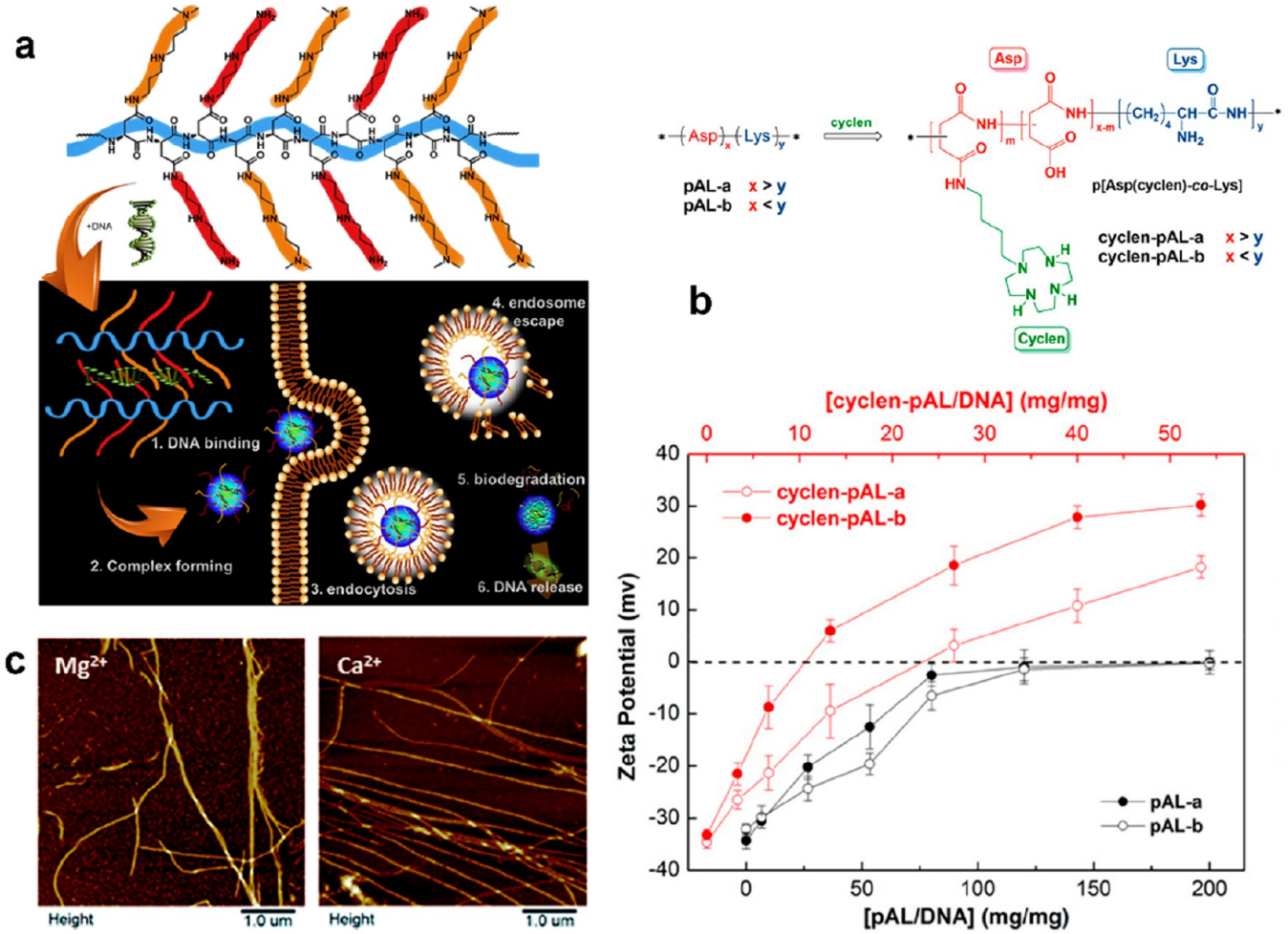

Figure 8. Loading and delivery of NAs. (a) Structure of the positively charged PASP and schematic illustration of the complex formation between the polymer and DNA, cell uptake, endocytosis, endosome escape, biodegradation, and release of DNA. Reproduced with permission from ref 142 Copyright 2013 Elsevier. (b) Grafting of cyclen to copolymers of PASP and lysine (top panel), and zeta-potential of the polymer/DNA complexes at different ratios (bottom panel). Reproduced with permission from ref 148. Copyright 2016 American Chemical Society. (c) AFM images of the one strand nanotubes prepared by self-assembly in Mg- and Ca-containing buffer solutions. Reproduced with permission from ref 151. Copyright 2019 Royal Society of Chemistry.

compared with that of PEG as negative control, which revealed that the serum resistance of the particles is as efficient as PEG.

Although the aforementioned coatings look highly promising, they lack a strong interaction with the substrate such as covalent bonds and thus may become inefficient in the long term. To ensure a permanent coating, coupling agents may be required to be incorporated into PASP. The type of modification depends on the functional groups of the substrate suitable for the reactions. As mentioned above, dopamine can be attached to virtually any kind of surface through catechol groups, whereas the amine groups can be served for conjugation to PASP.[139]

7.3. Mucoadhesion. Mucoadhesion is defined as the adhesion of synthetic or natural biomaterials to the mucus layer. Mucus is secreted from epithelial cells and is present in a variety of places such as the eyes, nose, and gastrointestinal (GI) tract.[140] Mucoadhesion in drug delivery systems is a viable strategy to improve drug bioavailability.[82] Among all available techniques, thiolation is considered to be a highly effective choice for improving mucoadhesion.[84] Thiolated molecules are believed to form covalent disulfide bonds with the cysteine moieties of the mucus glycoproteins, thereby improving mucoadhesion.[82−84]

Most studies regarding PASP mucoadhesion have been carried out for the development of ocular formulations through thiolation, which provides materials with in situ gelation properties and in turn a durable gel layer. Optimum transparency, surface tension, nontoxicity, resistance against blinking, gelation time, and mucoadhesion need to be achieved by tuning the material structure.[83] By incorporation of a high amount of thiols, PASP formulations capable of in situ gelling were developed with strong mucoadhesion in porcine conjunctiva.[29] The role of thiolation was clearly demonstrated by the increased adhesion of the hydrogel to mucus when its thiol content increased. Employing rheological measurements, Horvat et al.[76] found that the presence of mucin contributes to in situ gelation of the thiolated PASP, reduces time to gelation, and improves gel strength. The role of mucin was realized when polymer and oxidant concentration decreased, whereas at high concentration, its role was not noticeable. It is important to note that thiolated PASP can be subjected to premature gelation through oxidation upon exposure to air. Therefore, the use of a suitable antioxidant such as

https://doi.org/10.1021/acsbiomaterials.1c00150
ACS Biomater. Sci. Eng. XXXX, XXX, XXX−XXX

Table 4. Use of PASP and Its Derivatives through Modification with Amine-Containing Species in Different Drug Delivery Systems

physical structure	modification	loaded compounds	result	ref
hydrogel	CYS	diclofenac sodium (DFS)	Modification with CYS led to thiolation, improved muco-adhesion, and in situ gelation of the polymer by an oxidant. The DFS-loaded gels showed sustained release and were used as ophthalmic formulation.	76
hydrogel	cyclodextrin, PEG, and hydrazine	nicardipine hydrochloride (NIC)	Cyclodextrin was used for complex formation of the polymer with NIC (as a hydrophobic drug), whereas hydrazine was employed for in situ cross-linking with dextran aldehyde polymer (oxidized dextran) for gelation. Loading and release of NIC-loaded polymers were evaluated.	173
hydrogel	allyl amine	DFS	Allyl amine has a double bond and was employed for cross-linking of PASP polymer by radical copolymerization with *N*-isopropylacrylamide. The latter network alone has a temperature sensitivity around 32 °C. The prepared gels showed pH- and temperature-responsiveness and were studied for loading/release of DFS.	174
hydrogel	cyclodextrin and CYS	prednisolone	Cyclodextrin increased the hydrophobicity and improved prednisolone loading via complexation, whereas CYS provided the polymer with in situ gelation and muco-adhesion. Prolonged release of ophthalmic formulation was achieved.	175
hydrogel	3-aminopropyltriethoxysilane	salicylic acid	Silane coupling agent conjugated to PASP served as a cross-linker. Semi-interpenetrating polymer network (semi-IPN) with poly(vinyl alcohol) were prepared and salicylic acid release was evaluated.	176
injectable hydrogels	3-amino-1-propanol, and tyramine.	rhodamine B (Rh B)	The phenol groups of tyramine undergoe oxidative coupling in the presence of horseradish peroxidase (HRP) and hydrogen peroxide (H_2O_2), leading to cross-linking and in situ gelation. The gelation time of these injectable hydrogels were tuned from 10 s to 8 min by varying HRP and H_2O_2. Loading/release of Rh B as a model drug was assessed.	177
nanocarrier	folic acid and amylose	curcumin (CUR)	Amylose increased the complexation with poorly water-soluble CUR and protecting it from photodegradation. Folate conjugation was carried out to provide the carriers with folate targeting as cancer cells typically have folate receptors. The particles were assessed for loading/delivery of CUR.	178
nanocapsules	3-amino-1,2-propanediol (2-APD) and dimethylaminopropylamine (DMAPA) & hydrazine	BSA	Nanocapsules were prepared via layer-by-layer assembly of oppositely charged PASP and polyaspartamides (PASM) as shell on silica core followed by its removal. The two polymers were conjugated with aldehyde (from conversion of 2-APD) and hydrazine moieties for covalent cross-linking of the shell. Cationic PASM was prepared through DMAPA conjugation. The capsules were employed for BSA loading/release as a hydrophilic model drug.	179
nanogels	hydrazine, 2APD, DMAPA and 1,3-propane sultone	DOX	Similar to the reference,[179] hydrazone linkage was formed as aldehyde and hydrazine in the two polymers were reacted, leading to nanogel formation. Propane sultone was also conjugated to provide the nanogels with zwitterionic property. DOX loading/release was assessed.	72
nanogels	CYS	fluorescent dextran (FITC-Dx)	S−S cross-linking bonds as a result of polymer thiolation were cleaved in the presence of dithiothreitol (DTT) as a reducing agent, leading to fast release of FTIC-Dx as a model drug.	79
particles	cholic acid, m-PEG, and hydrazine	DOX	Cholic acid increased the polymer hydrophobicity and made it suitable for aggregate formation in water (particle size range: 125−200 nm). DOX was conjugated to the polymer backbone via hydrazone linkage, which can be cleaved in acidic media (e.g., intracellular), releasing DOX faster.	93
particles	lauryl amine, m-PEG, 2-diisopropylaminoethyl (DIP)	paclitaxel (PTX)	DIP and lauryl amine respectively made the polymer cationic and hydrophobic. m-PEG was also utilized for prolonged blood circulation. Nanoparticles (size range 100−120 nm) showed dissolution at acidic media due to the cationic nature of the polymer arising from DIP moiety. This led to faster release PTX from under acidic conditions (pH 6.5 vs pH 7.4).	27
particles	octadecylamine	DOX	Magnetic PASP nanoparticles prepared for DOX delivery, improving dispersion capability of iron oxide nanoparticles and T2 contrast enhancement.	88
micelles	CYS, hexamethylenediamine (HMDA), and mPEG-NH_2	DOX	PASP modification with CYS led to thiolation and subsequent cross-linking of the micelles with an oxidizing agent (thiol to disulfide transition upon oxidation/reduction reactions). HMDA and PEG were used for permanent cross-linking and for prolonging micelle circulation, respectively. DOX release was faster in the case of thiolated micelles and was triggered under reductive media.	78
micelles	phenylborate serine	DOX	Modification with phenylborate serine resulted in reactive oxygen species (ROS)-responsive carrier. The release study of DOX-loaded micelles showed that H_2O_2 increases the release rate.	180
micelles	2-phenylethylamine, and N-(3-aminopropyl)-imidazole, and MPEG-S2-NH_2	DOX	MPEG-S2-NH_2 was used as sheddable hydrophilic shell in a reductive environment due to S−S bonds. Such cleavage of the micelles led to fast release of DOX. 2-Phenylethylamine and N-(3-aminopropyl)-imidazole were used to increase hydrophobicity and improve pH-responsiveness, respectively.	43

https://doi.org/10.1021/acsbiomaterials.1c00150
ACS Biomater. Sci. Eng. XXXX, XXX, XXX−XXX

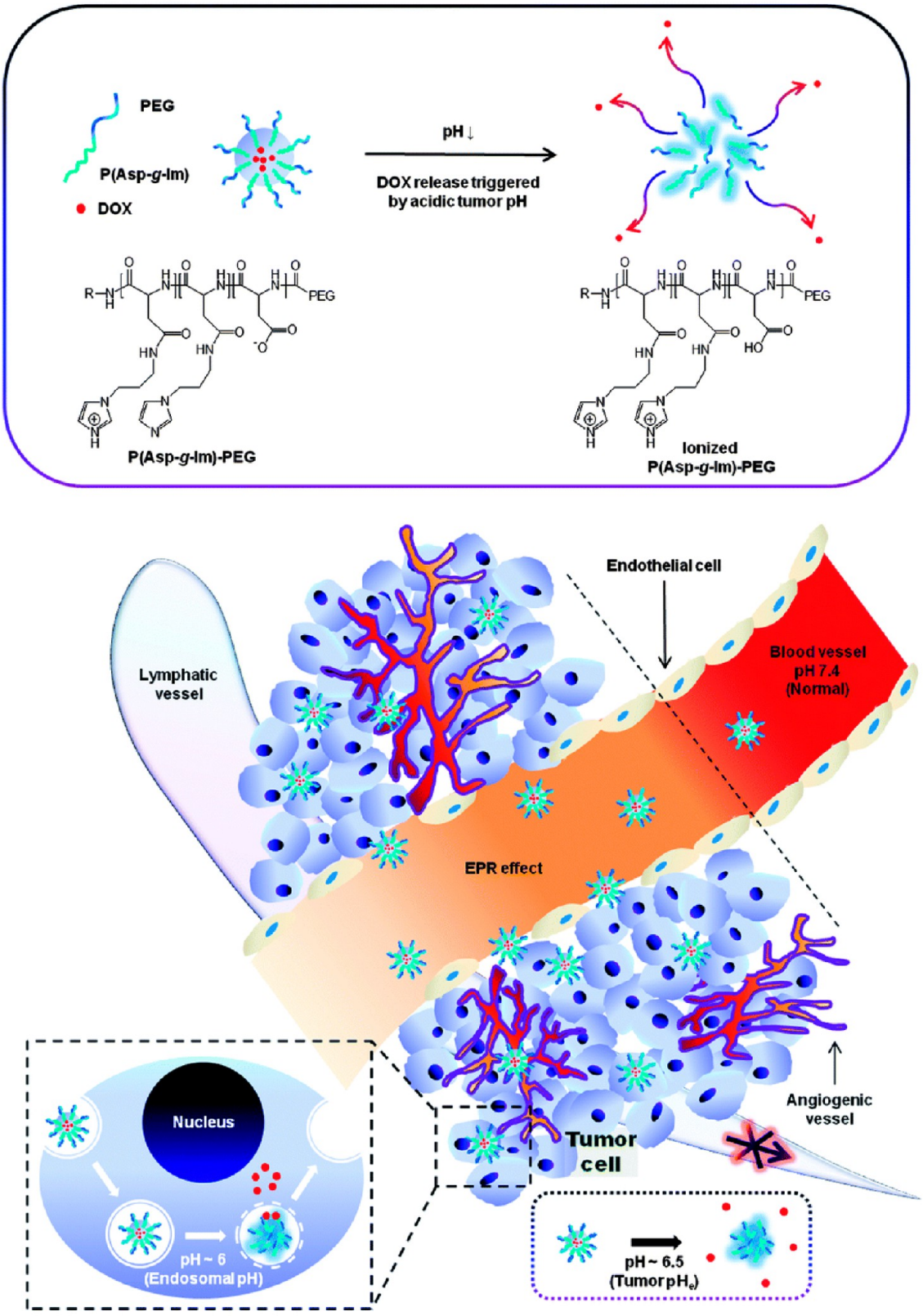

Figure 9. Schematic representation of the proposed concept of the modified PASP in the bloodstream (pH 7.4). Because of the hydrophobic imidazole groups as well as a PEG block on the surface, the micelles have prolonged and stable circulation in the bloodstream until they reach the vicinity of the tumor cells. Then, they will accumulate by the enhanced permeability and retention (EPR) effect, and subsequently the acidic microenvironment triggers the release of DOX. Reproduced with permission from ref 152. Copyright 2014 Royal Society of Chemistry.

acetylcysteine or dithiothreitol in the ocular formulations is necessary.[77]

7.4. Delivery of Nucleic Acids. The delivery of nucleic acids (e.g., DNA and siRNA) to cells can be challenging

https://doi.org/10.1021/acsbiomaterials.1c00150
ACS Biomater. Sci. Eng. XXXX, XXX, XXX−XXX

because they are negatively charged and thus are repelled by the negatively charged cell surfaces. Therefore, cationic polymers are usually used to load the NAs through electrostatic attraction.[141] This also protects the nucleic acids payload from degradation. By tuning the overall charge of the carrier to positive, one can induce intracellular delivery of the NA payload.[141] As seen in Figure 8a, the complex enters the cell via endocytosis, followed by endosomal escape and the release of DNA.[142]

Introduction of amine groups into the PASP can lead to a positively charged polymer and thus presents a suitable candidate for loading of NAs.[143] PASP-based polymers modified with cyclodextrin and cationic amine groups were shown to possess much better plasmid DNA transfection compared to polyethylenimine.[144] Polyethylenimine is a widely used and efficient polymer for NA condensation and transfection and has high efficiency.[90] However, in terms of toxicity and degradability, PASP-based carriers are superior to pure polyethylenimine.[145] Therefore, the combination of ethylenimine oligomers with PASP through conjugation may offer promising results for NA loading and delivery.[142,146] Dong et al.[89] designed multiarmed PASP grafted with ethylenimine oligomers (size 90−150 nm, positive zeta potential of 25 to 40 mV), which showed good NA condensation and gene transfection activity.

PASP modification for NA transfection purposes has also been carried out with other moieties. For example, Salakheiva et al.[147] employed (dialkylamino)alkyl and alkyl or hydroxyalkyl and evaluated the role of the structure and degree of incorporation of these pendant groups on transfection. The disadvantage of the prepared carriers was their resistance against serum-induced aggregation, leading to low transfection efficiency in serum. In another study, Ma et al.[148] showed that grafting of cyclen molecules on poly(ASP-*co*-lysine) significantly enhances DNA transfection efficiency while not affecting cell viability. Cyclen has recently been the subject of many studies due to interactions with NAs.[149] As seen in Figure 8-b, increasing the polymer/DNA weight ratio increased zeta potential to positive values and decreased the size of the complex (to around 100 nm). The optimum range of the polymer/DNA ratio was found to be around 20−50 for the DNA to be efficiently compacted into small nanoparticles.

Cationic modification of PASP by hydrophobic groups (trimethylammonium-based) has also revealed that an increasing alkyl chain length improves transfection efficiency of DNA.[150] The prepared cationic polymers were self-assembled with DNA and then coated with Na-PASP. The complexes were used for oral delivery of DNA in a murine colitis model, which led to a significant reduction of gut inflammation.

In another effort to stimulate enamel regeneration through biomimetic mineralization, conjugates of DNA-PASP were prepared and self-assembled by magnesium (Mg)- as well as Ca-containing buffer solutions into ordered nanotubes (shown in Figure 8-c).[151] Such self-assembly can potentially pave the way for tuning guided HAp mineralization in vivo.

7.5. Drug Delivery. Drug delivery by a suitable carrier to the affected sites can effectively lower its side effects on healthy tissues while protecting the drug from degradation and improving its efficacy. The carrier may be in different physical forms such as micelles,[152] liposomes,[153] particles,[154] hydrogels,[155] or bulk polymer[155,156] and is designed on the basis of the administration route, drug chemistry, and the required release rate. The carrier can also protect the therapeutic agent from aggressive environments (e.g., acidic and enzyme-rich media of the GI tract).[157] The core requirements of the drug carrier are biocompatibility and biodegradability which PASP and its derivatives enjoy due to a protein-like peptide backbone. In addition, because of facile modification, a wide variety of species can be conjugated to PASP to tailor a carrier for a given drug as summarized in Table 4.

Despite all the advantages, the hydrophilicity of PASP prevents loading of lipophilic drugs, which limits its application. Several studies have focused on the modification of PASP through either grafting or copolymerization to address this limitation.[76,77] For example, PASP was modified with cyclodextrin to enable loading of prednisolone, a lipophilic ophthalmic drug.[84] Cyclodextrin forms a strong complex with the drug, and prolongs its release. Incorporation of lactic acid as a comonomer to PASP can also increase hydrophobicity.[42,50,51] 1,2-dipalmitoyl-*sn*-glycero-3-phosphoethanolamine (DPPE) was grafted to the PASP-poly(lactic acid) copolymers to further improve biocompatibility, extend half-life circulation and to increase drug loading. The modified polymer was then loaded with doxorubicin (DOX) through a double emulsion and delivered to a murine cancer model. DOX-loaded particles were more effective in terms of inhibition of tumor growth, toxicity, and mortality when compared to free DOX.[50]

Because of pendant carboxylic acid groups, PASP is regarded as a pH-sensitive polymer, adopting collapsed and extended chain conformation in acidic and basic media, respectively. The transition pH at which chain conformation occurs can be tuned by incorporation of other ionic functional groups. For instance, Lee et al.[152] grafted imidazole to PASP-*b*-PEG copolymers (60% with respect to the polymer weight), resulting in a pH-sensitive zwitterionic micelle, which could achieve a high DOX loading of 28% (Figure 9). At pH 7.4, imidazole-PASP block is hydrophobic due to the deprotonation of imidazole while PEG block is hydrophilic, providing amphiphilicity to form micelle structure. PEG also provides micelle stability in the bloodstream against opsonization. It was postulated that the micelles can accumulate in the tumor through the enhanced permeability and retention (EPR) effect. The acidic microenvironment around the tumor is believed to lead to the amine protonation of imidazole, and subsequent micelle dissociation, thereby triggering DOX release. In addition, cellular uptake can also provide an acidic endosomal environment for micelle rupture and DOX release (endosomal pH <6.5).

Redox-responsiveness can also be added to PASP through thiolation. Park et al.[78] showed that thiolated PASP nanogels cross-linked by disulfide bonds can completely dissolve under reductive conditions. To maintain structural integrity of the particles, Krisch et al.[81] added a permanent cross-linker and showed the pH- and redox-responsiveness of the nanogels. The particle size increased from 141 to 216 nm after exposing the particles to a reducing agent (Figure 5c) which is an interesting feature for the release of bioactive payloads.

Targeted delivery of drugs to specific parts of the body is a desirable characteristic of engineered carriers. Facile conjugation of targeting agents (e.g., antibodies, and peptides) to PASP can be highly advantageous in this regard. For instance, PASP modified with dopamine and octadecyl amine were successfully employed as carriers (100−300 nm) for targeted delivery of curcumin, camptothecin and DOX to the human colon adenocarcinoma cells.[85] High targeting efficiency was

https://doi.org/10.1021/acsbiomaterials.1c00150
ACS Biomater. Sci. Eng. XXXX, XXX, XXX−XXX

achieved because the particles had dopamine pendant groups which could be recognized by dopamine receptors expressed on the surface of the cells. In another study, folic acid and amylose were grafted to PASP to enhance the curcumin loading and to simultaneously provide the polymer with folate- and glycol-targeting.[158]

The combination of metal and metal oxide particles such as iron oxide[159] and silver[160] with polymers can expand uses in biomedical applications. Iron oxide, which is extensively employed for the enhancement of MRI,[161−171] is relatively toxic. The use of PASP−PEG copolymers as a stabilizer for such particles reduces the toxicity significantly.[159] Aside from biocompatibility, improved MRI was achieved when iron oxide was incorporated into PASP-based particles loaded with DOX.[88] Furthermore, it has interestingly been revealed that pure PASP can function both as an efficient reducing and stabilizing agent for the synthesis of gold nanoparticles (AuNPs).[172] The synthesized PASP-stabilized AuNPs (size of ca. 55 nm) were then loaded with a high amount of DOX and administered to fibrosarcoma induced mice, which showed much better antitumor efficiency when compared to free DOX.

7.6. Bone Targeting and Biomineralization. Treatment of bone-related diseases is quite challenging because of low blood flow in the tissues surrounding bone.[181] Thus, targeted delivery of bioactive agents could be of great importance. The main component of bone is hydroxyapatite (HAp) (ca. 70%), which has a high affinity with ASP and PASP. This affinity originates from the calcium chelation of PASP and ASP, and the formation of strong complexes with calcium. As such, PASP has been widely utilized as an efficient antiscalant in different industries where precipitation/deposition of salts of calcium (e.g., calcium phosphate) is detrimental to water flow.[182] In biomedical areas, however, the affinity of PASP and ASP to calcium has been exploited for targeting of various forms of drug-containing carriers to bone.[9−12]

The targeting efficacy of ASP groups to bone was confirmed in vitro and in vivo when it was conjugated to PLGA−PEG particles.[10] In addition, conjugation of PASP to PTX-loaded liposomes was shown to significantly improve bone targeting and treatment efficiency in metastatic tumor mouse models.[166] Fluorescent tagging of the liposomes showed that they accumulated mostly on the eroded bone surfaces. The optimum ASP repeating unit number was found to be from 4 to 10 for an effective bone−ASP interaction.[183−185]

Osteopontin (OPN), an anionic phosphoprotein that is rich in ASP moiety (approximately 15−20%) and contributes in many biomineralization processes, has been found to be a natural inhibitor for vascular calcification, as well as formation of kidney stones. In vascular calcification, HAp salts mineralize in the vessel walls via a process mediated by smooth muscle cells. This is due mainly to hypercalcemia and hyperphosphatemia, which eventually leads to blood vessel stiffening. Giachelli et al.[186] showed that OPN prevents HAp nucleation and growth and thus blocks vascular calcification. Regarding kidney stones which are usually made up of calcium oxalate monohydrate, low levels of OPN in urine is regarded as a risk factor for their formation.[187] The inhibition property in these cases is attributed to the presence ASP repeating units and the acidic nature of OPN.[187]

8. CONCLUSION AND PROSPECTS

PASP and its derivatives have biocompatibility and biodegradability similar to that of polypeptides. They also have a strong affinity with calcium ions, opening a wide window for their use in biomineralization and bone-related areas. Facile modification of PAPS allows one to customize the material for variety of biomedical applications ranging from delivery of bioactive agents to development of scaffolds. Conjugation of variety of species such as dopamine, long alkyl chain, and thiol is reviewed in this paper. Overall, these features are expected to result in the development of even more novel PASP-based biomaterials in the future. For instance, thanks to strong calcium chelation, PASP may be utilized for inhibition of ectopic calcification of soft tissues. Because of significant enhancement of mucoadhesion via thiolation, PASP also possesses the potential to be studied for oral administration of susceptible drugs. Because of the hydrolysis of PSI to PASP under physiological conditions, the former may be directly exploited for the design of delivery systems as well. Furthermore, facile modification may attract more attention in terms of conjugation of drug and targeting molecules to PASP in the delivery systems. The combination of reducing, stabilizing, and chelation abilities of PASP collectively can be exploited for the efficient synthesis of various metallic nanoparticles (e.g., gold and silver). In terms of biomedical diagnosis, PASP has recently shown to stabilize iron oxide nanoparticles and reduce their toxicity, necessitating more investigation for more efficient MRI imaging. Despite assessing the effect of different enzymes and bacteria, there is still no study on in vivo degradation and retention of PASP. Such studies would be highly useful considering biomedical applications of PASP. In summary, the interest in PASP is increasingly growing, potentially unveiling even more interesting biomedical applications in the future.

AUTHOR INFORMATION

Corresponding Author

Hang T. Ta − *Queensland Micro- and Nanotechnology and School of Environment and Science, Griffith University, Nathan, Queensland 4111, Australia; Australian Institute for Bioengineering and Nanotechnology, The University of Queensland, St Lucia, Queensland 4072, Australia;* orcid.org/0000-0003-1188-0472; Email: h.ta@griffith.edu.au

Authors

Hossein Adelnia − *Australian Institute for Bioengineering and Nanotechnology and School of Pharmacy, Pharmacy Australia Centre of Excellence, The University of Queensland, St Lucia, Queensland 4072, Australia; Queensland Micro- and Nanotechnology, Griffith University, Nathan, Queensland 4111, Australia*

Huong D.N. Tran − *Australian Institute for Bioengineering and Nanotechnology, The University of Queensland, St Lucia, Queensland 4072, Australia; Queensland Micro- and Nanotechnology, Griffith University, Nathan, Queensland 4111, Australia*

Peter J. Little − *School of Pharmacy, Pharmacy Australia Centre of Excellence, The University of Queensland, Woolloongabba, Queensland 4012, Australia; Sunshine Coast Health Institute, University of the Sunshine Coast, Birtinya, Queensland 4575, Australia*

Idriss Blakey − *Australian Institute for Bioengineering and Nanotechnology, The University of Queensland, St Lucia, Queensland 4072, Australia; Centre for Advanced Imaging,*

https://doi.org/10.1021/acsbiomaterials.1c00150
ACS Biomater. Sci. Eng. XXXX, XXX, XXX−XXX

University of Queensland, Brisbane, Queensland 4067, Australia; orcid.org/0000-0003-2389-6156

Complete contact information is available at: https://pubs.acs.org/10.1021/acsbiomaterials.1c00150

Author Contributions

H.A. wrote the manuscript. I.B. and P.J.L. revised the manuscript. H.T.T. provided supervision and revised the manuscript.

Notes

The authors declare no competing financial interest.

■ ACKNOWLEDGMENTS

This work is funded by National Health and Medical Research Council (HTT: APP1037310, APP1182347, APP2002827), Heart Foundation (HTT: 102761), and the University of Queensland (HA, HDNT: Research Training Scholarship).

■ REFERENCES

(1) Meka, V. S.; Sing, M. K.; Pichika, M. R.; Nali, S. R.; Kolapalli, V. R.; Kesharwani, P. A comprehensive review on polyelectrolyte complexes. *Drug Discovery Today* **2017**, *22* (11), 1697−1706.

(2) Molaei, S. M.; Adelnia, H.; Seif, A. M.; Nasrollah Gavgani, J. Sulfonate-functionalized polyacrylonitrile-based nanoparticles; synthesis, and conversion to pH-sensitive nanogels. *Colloid Polym. Sci.* **2019**, *297* (9), 1245−1253.

(3) Alam, A. U.; Qin, Y.; Nambiar, S.; Yeow, J. T.; Howlader, M. M.; Hu, N.-X.; Deen, M. J. Polymers and organic materials-based pH sensors for healthcare applications. *Prog. Mater. Sci.* **2018**, *96*, 174−216.

(4) Mohamed, R. R.; Elella, M. H. A.; Sabaa, M. W. Cytotoxicity and metal ions removal using antibacterial biodegradable hydrogels based on N-quaternized chitosan/poly (acrylic acid). *Int. J. Biol. Macromol.* **2017**, *98*, 302−313.

(5) Jalalvandi, E.; Shavandi, A. Polysuccinimide and its derivatives: degradable and water soluble polymers. *Eur. Polym. J.* **2018**, *109*, 43−54.

(6) Yavvari, P. S.; Awasthi, A. K.; Sharma, A.; Bajaj, A.; Srivastava, A. Emerging biomedical applications of polyaspartic acid-derived biodegradable polyelectrolytes and polyelectrolyte complexes. *J. Mater. Chem. B* **2019**, *7* (13), 2102−2122.

(7) Robla-Alvarez, S.; Alonso, M. J.; Csaba, N. Polyaminoacid-based nanocarriers: a review of the latest candidates for oral drug delivery. *Expert Opin. Drug Deliv.* **2020**, 1081.

(8) Ganguly, A.; Sharma, K.; Majumder, K., Peptides as biopolymers—past, present, and future. In *Biopolymer-Based Formulations*; Elsevier: 2020; pp 87−104.

(9) Lotsari, A.; Rajasekharan, A. K.; Halvarsson, M.; Andersson, M. Transformation of amorphous calcium phosphate to bone-like apatite. *Nat. Commun.* **2018**, *9*, 4170.

(10) Fu, Y.-C.; Fu, T.-F.; Wang, H.-J.; Lin, C.-W.; Lee, G.-H.; Wu, S.-C.; Wang, C.-K. Aspartic acid-based modified PLGA-PEG nanoparticles for bone targeting: In vitro and in vivo evaluation. *Acta Biomater.* **2014**, *10* (11), 4583−4596.

(11) Jiang, T.; Yu, X.; Carbone, E. J.; Nelson, C.; Kan, H. M.; Lo, K. W.-H. Poly aspartic acid peptide-linked PLGA based nanoscale particles: potential for bone-targeting drug delivery applications. *Int. J. Pharm.* **2014**, *475* (1−2), 547−557.

(12) Rotman, S. G.; Moriarty, T. F.; Nottelet, B.; Grijpma, D. W.; Eglin, D.; Guillaume, O. Poly (Aspartic Acid) Functionalized Poly (ϵ-Caprolactone) Microspheres with Enhanced Hydroxyapatite Affinity as Bone Targeting Antibiotic Carriers. *Pharmaceutics* **2020**, *12* (9), 885.

(13) Nayunigari, M. K.; Gupta, S. K.; Kokkarachedu, V.; Kanny, K.; Bux, F. Development of anti-scale poly (aspartic acid-citric acid) dual polymer systems for water treatment. *Environ. Technol.* **2014**, *35* (23), 2903−2909.

(14) Zhang, S.; Qu, H.; Yang, Z.; Fu, C.-E.; Tian, Z.; Yang, W. Scale inhibition performance and mechanism of sulfamic/amino acids modified polyaspartic acid against calcium sulfate. *Desalination* **2017**, *419*, 152−159.

(15) Feng, J.; Gao, L.; Wen, R.; Deng, Y.; Wu, X.; Deng, S. Fluorescent polyaspartic acid with an enhanced inhibition performance against calcium phosphate. *Desalination* **2014**, *345*, 72−76.

(16) Low, K. C.; Wheeler, A.; Koskan, L. P. Commercial poly (aspartic acid) and its uses. *Adv. Chem. Ser.* **1996**, *248*, 99−112.

(17) Wolk, S. K.; Swift, G.; Paik, Y. H.; Yocom, K. M.; Smith, R. L.; Simon, E. S. One-and two-dimensional nuclear magnetic resonance characterization of poly (aspartic acid) prepared by thermal polymerization of L-aspartic acid. *Macromolecules* **1994**, *27* (26), 7613−7620.

(18) Tomida, M.; Nakato, T.; Matsunami, S.; Kakuchi, T. Convenient synthesis of high molecular weight poly (succinimide) by acid-catalysed polycondensation of L-aspartic acid. *Polymer* **1997**, *38* (18), 4733−4736.

(19) Bossion, A.; Heifferon, K. V.; Meabe, L.; Zivic, N.; Taton, D.; Hedrick, J. L.; Long, T. E.; Sardon, H. Opportunities for organocatalysis in polymer synthesis via step-growth methods. *Prog. Polym. Sci.* **2019**, *90*, 164−210.

(20) Adelnia, H.; Gavgani, J. N.; Soheilmoghaddam, M. Fabrication of composite polymer particles by stabilizer-free seeded polymerization. *Colloid Polym. Sci.* **2015**, *293* (8), 2445−2450.

(21) Nakato, T.; Kusuno, A.; Kakuchi, T. Synthesis of poly (succinimide) by bulk polycondensation of L-aspartic acid with an acid catalyst. *J. Polym. Sci., Part A: Polym. Chem.* **2000**, *38* (1), 117−122.

(22) Zrinyi, M.; Gyenes, T.; Juriga, D.; Kim, J.-H. Volume change of double cross-linked poly (aspartic acid) hydrogels induced by cleavage of one of the crosslinks. *Acta Biomater.* **2013**, *9* (2), 5122−5131.

(23) Kokufuta, E.; Suzuki, S.; Harada, K. Temperature effect on the molecular weight and the optical purity of anhydropolyaspartic acid prepared by thermal polycondensation. *Bull. Chem. Soc. Jpn.* **1978**, *51* (5), 1555−1556.

(24) Adelnia, H.; Nasrollah Gavgani, J.; Riazi, H.; Cheraghi Bidsorkhi, H. Transition behavior, surface characteristics and film formation of functionalized poly (methyl methacrylate-co-butyl acrylate) particles. *Prog. Org. Coat.* **2014**, *77* (11), 1826−1833.

(25) Tomida, M.; Nakato, T.; Matsunami, S.; Kakuchi, T. Convenient synthesis of high molecular weight poly (succinimide) by acid-catalysed polycondensation of L-aspartic acid. *J. Polym. Sci., Part A: Polym. Chem.* **1997**, *38* (18), 4733−4736.

(26) Nakato, T.; Yoshitake, M.; Matsubara, K.; Tomida, M.; Kakuchi, T. Relationships between structure and properties of poly (aspartic acid) s. *Macromolecules* **1998**, *31* (7), 2107−2113.

(27) Moon, J. R.; Jeon, Y. S.; Zrinyi, M.; Kim, J.-H. pH-Responsive PEGylated nanoparticles based on amphiphilic polyaspartamide: preparation, physicochemical characterization and in vitro evaluation. *Polym. Int.* **2013**, *62* (8), 1218−1224.

(28) Kang, H. S.; Yang, S. R.; Kim, J.-D.; Han, S.-H.; Chang, I.-S. Effects of grafted alkyl groups on aggregation behavior of amphiphilic poly (aspartic acid). *Langmuir* **2001**, *17* (24), 7501−7506.

(29) Szilágyi, B. Á.; Gyarmati, B.; Horvát, G.; Laki, Á.; Budai-Szüücs, M.; Csányi, E.; Sandri, G.; Bonferoni, M. C.; Szilágyi, A. The effect of thiol content on the gelation and mucoadhesion of thiolated poly (aspartic acid). *Polym. Int.* **2017**, *66* (11), 1538−1545.

(30) Zakharchenko, S.; Sperling, E.; Ionov, L. Fully biodegradable self-rolled polymer tubes: a candidate for tissue engineering scaffolds. *Biomacromolecules* **2011**, *12* (6), 2211−2215.

(31) Koskan, L. P.; Meah, A. R. Production of high molecular weight polysuccinimide and high molecular weight polyaspartic acid from maleic anhydride and ammonia. Patent US5219952A, 1993.

(32) Boehmke, G.; Schmitz, G. Process for the preparation of polysuccinimide, polyaspartic acid and their salts. Paent US5610255A, 1995.
(33) Wood, L. L., Preparation of salt of polyaspartic acid by high temperature reaction. Patent US5367047A, 1994.
(34) Ni, L.; Chiriac, A.; Popescu, C.; Neam, I. Possibilities for poly (aspartic acid) preparation as biodegradable compound. *J. Optoelectron. Adv. Mater.* **2006**, *8* (2), 663−666.
(35) Shi, S.; Zhao, X.; Wang, Q.; Shan, H.; Xu, Y. Synthesis and evaluation of polyaspartic acid/furfurylamine graft copolymer as scale and corrosion inhibitor. *RSC Adv.* **2016**, *6* (104), 102406−102412.
(36) Boehmke, G. Polyaspartic acid from maleic acid and ammonia. Patent US4839461A, 1989.
(37) Huang, J. L.; Zhang, Y. L.; Cheng, Z. H.; Tao, H. C. Microwave-assisted synthesis of polyaspartic acid and its effect on calcium carbonate precipitate. *J. Appl. Polym. Sci.* **2007**, *103* (1), 358−364.
(38) Freeman, M. B.; Paik, Y. H.; Simon, E. S.; Swift, G. Production of polysuccinimide by thermal polymerization of maleamic acid. Patent EP0593187A1, 1995.
(39) Fukumura, K.; Kuboi, H.; Fukuda, K. Methods for producing polyaspartic acid precursor polymer and polyaspartic acid salt. Patent US9096720B2, 2015.
(40) Shi, S.; Zhao, X.; Wang, Q.; Shan, H.; Xu, Y. Synthesis and evaluation of polyaspartic acid/furfurylamine graft copolymer as scale and corrosion inhibitor. *RSC Adv.* **2016**, *6* (104), 102406−102412.
(41) Masayuki, Y.; Mizue, M.; Noriko, Y.; Teruo, O.; Yasuhisa, S.; Kazunori, K.; Shohei, I. Polymer micelles as novel drug carrier: adriamycin-conjugated poly (ethylene glycol)-poly (aspartic acid) block copolymer. *J. Controlled Release* **1990**, *11* (1−3), 269−278.
(42) Tudorachi, N.; Lipsa, R.; Vasile, C.; Mustata, F. Poly (lactic acid)-co-aspartic acid copolymers: possible utilization in drug delivery systems. *J. Polym. Environ.* **2013**, *21* (4), 1064−1071.
(43) Gong, C.; Shan, M.; Li, B.; Wu, G. A pH and redox dual stimuli-responsive poly (amino acid) derivative for controlled drug release. *Colloids Surf., B* **2016**, *146*, 396−405.
(44) Kumagai, M.; Imai, Y.; Nakamura, T.; Yamasaki, Y.; Sekino, M.; Ueno, S.; Hanaoka, K.; Kikuchi, K.; Nagano, T.; Kaneko, E.; et al. Iron hydroxide nanoparticles coated with poly (ethylene glycol)-poly (aspartic acid) block copolymer as novel magnetic resonance contrast agents for in vivo cancer imaging. *Colloids Surf., B* **2007**, *56* (1−2), 174−181.
(45) Sanada, Y.; Akiba, I.; Hashida, S.; Sakurai, K.; Shiraishi, K.; Yokoyama, M.; Yagi, N.; Shinohara, Y.; Amemiya, Y. Composition dependence of the micellar architecture made from poly (ethylene glycol)-block-poly (partially benzyl-esterified aspartic acid). *J. Phys. Chem. B* **2012**, *116* (28), 8241−8250.
(46) Silva, M.; Lara, A.; Leite, C.; Ferreira, E. Potential Tuberculostatic Agents: Micelle-Forming Copolymer Poly (ethylene glycol)-Poly (aspartic acid) Prodrug with Isoniazid. *Arch. Pharm.* **2001**, *334* (6), 189−193.
(47) Aoyagi, T.; Sugi, K.-I.; Sakurai, Y.; Okano, T.; Kataoka, K. Peptide drug carrier: studies on incorporation of vasopressin into nano-associates comprising poly (ethylene glycol)-poly (L-aspartic acid) block copolymer. *Colloids Surf., B* **1999**, *16* (1−4), 237−242.
(48) Park, C. W.; Yang, H.-M.; Lee, H. J.; Kim, J.-D. Core-shell nanogel of PEG-poly (aspartic acid) and its pH-responsive release of rh-insulin. *Soft Matter* **2013**, *9* (6), 1781−1788.
(49) Park, C. W.; Lee, H. J.; Yang, H. M.; Woo, M. A.; Park, H. G.; Kim, J. D. Size and morphology controllable core cross-linked self-aggregates from poly (ethylene glycol-b-succinimide) copolymers. *J. Polym. Sci., Part A: Polym. Chem.* **2011**, *49* (1), 203−210.
(50) Han, S.; Liu, Y.; Nie, X.; Xu, Q.; Jiao, F.; Li, W.; Zhao, Y.; Wu, Y.; Chen, C. Efficient Delivery of Antitumor Drug to the Nuclei of Tumor Cells by Amphiphilic Biodegradable Poly (L-Aspartic Acid-co-Lactic Acid)/DPPE Co-Polymer Nanoparticles. *Small* **2012**, *8* (10), 1596−1606.
(51) Han, S.; Wang, H.; Liang, X.; Hu, L.; Li, M.; Wu, Y. Nanoparticle carriers based on copolymers of poly (l-aspartic acid co-l-lactide)-1, 2-dipalmitoyl-sn-glycero-3-phosphoethanolamine for drug delivery. *J. Nanopart. Res.* **2011**, *13* (9), 4371−4385.
(52) Ye, R. R.; Wang, Z. Y.; Wang, Q. F.; Yang, K.; Luo, S. H. Synthesis of biodegradable material poly (lactic acid-co-aspartic acid) via direct melt polycondensation and its characterization. *J. Appl. Polym. Sci.* **2011**, *121* (6), 3662−3668.
(53) Shinoda, H.; Asou, Y.; Suetsugu, A.; Tanaka, K. Synthesis and Characterization of Amphiphilic Biodegradable Copolymer, Poly (aspartic acid-co-lactic acid). *Macromol. Biosci.* **2003**, *3* (1), 34−43.
(54) Mithil Kumar, N.; Gupta, S. K.; Jagadeesh, D.; Kanny, K.; Bux, F. Development of poly (aspartic acid-co-malic acid) composites for calcium carbonate and sulphate scale inhibition. *Environ. Technol.* **2015**, *36* (10), 1281−1290.
(55) Oyama, H. T.; Kimura, M.; Nakamura, Y.; Ogawa, R. Environmentally safe bioadditive allows degradation of refractory poly (lactic acid) in seawater: Effect of poly (aspartic acid-co-l-lactide) on the hydrolytic degradation of PLLA at different salinity and pH conditions. *Polym. Degrad. Stab.* **2020**, *178*, 109216.
(56) Migahed, M.; Rashwan, S.; Kamel, M.; Habib, R. Synthesis, characterization of polyaspartic acid-glycine adduct and evaluation of their performance as scale and corrosion inhibitor in desalination water plants. *J. Mol. Liq.* **2016**, *224*, 849−858.
(57) Lim, S. L.; Tang, W. N. H.; Ooi, C. W.; Chan, E. S.; Tey, B. T., Rapid swelling and deswelling of semi-interpenetrating network poly (acrylic acid)/poly (aspartic acid) hydrogels prepared by freezing polymerization. *J. Appl. Polym. Sci.* **2016**, *133* (24), DOI: 10.1002/app.43515.
(58) Liu, C.; Chen, Y.; Chen, J. Synthesis and characteristics of pH-sensitive semi-interpenetrating polymer network hydrogels based on konjac glucomannan and poly (aspartic acid) for in vitro drug delivery. *Carbohydr. Polym.* **2010**, *79* (3), 500−506.
(59) Zhang, C.; Wu, S.; Qin, X. Facile fabrication of novel pH-sensitive poly (aspartic acid) hydrogel by crosslinking nanofibers. *Mater. Lett.* **2014**, *132*, 393−396.
(60) Chen, J.; Xu, L.; Han, J.; Su, M.; Wu, Q. Synthesis of modified polyaspartic acid and evaluation of its scale inhibition and dispersion capacity. *Desalination* **2015**, *358*, 42−48.
(61) Gao, Y.; Fan, L.; Ward, L.; Liu, Z. Synthesis of polyaspartic acid derivative and evaluation of its corrosion and scale inhibition performance in seawater utilization. *Desalination* **2015**, *365*, 220−226.
(62) Zhang, C.; Wan, L. Y.; Wu, S.; Wu, D.; Qin, X.; Ko, F. A reversible colorimetric chemosensor for naked-eye detection of copper ions using poly (aspartic acid) nanofibrous hydrogel. *Dyes Pigm.* **2015**, *123*, 380−385.
(63) Jalalvandi, E.; Cabral, J.; Hanton, L. R.; Moratti, S. C. Cyclodextrin-polyhydrazine degradable gels for hydrophobic drug delivery. *Mater. Sci. Eng., C* **2016**, *69*, 144−153.
(64) Tudorachi, N.; Chiriac, A. P. TGA/FTIR/MS study on thermal decomposition of poly (succinimide) and sodium poly (aspartate). *Polym. Test.* **2011**, *30* (4), 397−407.
(65) Ghasemi, M.; Larson, R. G. Role of Electrostatic Interactions in Charge Regulation of Weakly Dissociating Polyacids. *Prog. Polym. Sci.* **2020**, 101322.
(66) Klein, T.; Klausa, T.; Elschner, A.; Moritz, R.-J.; Cordes, M. Polyaspartic acid concentration determination by fluorometry. US6989274B2, 2006.
(67) Patil, M.; Rajput, S. Succinimides: Synthesis, reaction and biological activity. *Int. J. Pharm. Pharm. Sci.* **2014**, *6* (11), 8−14.
(68) Adelnia, H.; Blakey, I.; Little, P. J.; Ta, H. T. Hydrogels Based on Poly (aspartic acid): Synthesis and Applications. *Front. Chem.* **2019**, *7*, 755.
(69) Gyenes, T.; Torma, V.; Gyarmati, B.; Zrínyi, M. Synthesis and swelling properties of novel pH-sensitive poly (aspartic acid) gels. *Acta Biomater.* **2008**, *4* (3), 733−744.
(70) Yu, H.; Sun, J.; Zhang, Y.; Zhang, G.; Chu, Y.; Zhuo, R.; Jiang, X. pH-and β-cyclodextrin-responsive micelles based on polyaspartamide derivatives as drug carrier. *J. Polym. Sci., Part A: Polym. Chem.* **2015**, *53* (11), 1387−1395.

https://doi.org/10.1021/acsbiomaterials.1c00150
ACS Biomater. Sci. Eng. XXXX, XXX, XXX−XXX

(71) Shen, Z.; Zhi, X.; Zhang, P. Preparation of fluorescent polyaspartic acid and evaluation of its scale inhibition for CaCO3 and CaSO4. *Polym. Adv. Technol.* **2017**, *28* (3), 367−372.
(72) Lu, C.; Li, B.; Liu, N.; Wu, G.; Gao, H.; Ma, J. A hydrazone crosslinked zwitterionic polypeptide nanogel as a platform for controlled drug delivery. *RSC Adv.* **2014**, *4* (92), 50301−50311.
(73) Meng, H.; Zhang, X.; Sun, S.; Tan, T.; Cao, H. Preparation of γ-aminopropyltriethoxysilane cross-linked poly (aspartic acid) superabsorbent hydrogels without organic solvent. *J. Biomater. Sci., Polym. Ed.* **2016**, *27* (2), 133−143.
(74) Jedlovszky-Hajdu, A.; Molnar, K.; Nagy, P. M.; Sinko, K.; Zrinyi, M. Preparation and properties of a magnetic field responsive three-dimensional electrospun polymer scaffold. *Colloids Surf., A* **2016**, *503*, 79−87.
(75) Budai-Szücs, M.; Horvát, G.; Gyarmati, B.; Szilágyi, B. Á.; Szilagyi, A.; Csihi, T.; Berkó, S.; Szabó-Révész, P.; Mori, M.; Sandri, G.; et al. In vitro testing of thiolated poly (aspartic acid) from ophthalmic formulation aspects. *Drug Dev. Ind. Pharm.* **2016**, *42* (8), 1241−1246.
(76) Horvát, G.; Gyarmati, B.; Berkó, S.; Szabó-Révész, P.; Szilágyi, B. Á.; Szilágyi, A.; Soós, J.; Sandri, G.; Bonferoni, M. C.; Rossi, S.; et al. Thiolated poly (aspartic acid) as potential in situ gelling, ocular mucoadhesive drug delivery system. *Eur. J. Pharm. Sci.* **2015**, *67*, 1−11.
(77) Budai-Szücs, M.; Horvát, G.; Gyarmati, B.; Szilágyi, B. Á.; Szilágyi, A.; Berkó, S.; Ambrus, R.; Szabó-Révész, P.; Sandri, G.; Bonferoni, M. C.; et al. The effect of the antioxidant on the properties of thiolated poly (aspartic acid) polymers in aqueous ocular formulations. *Eur. J. Pharm. Biopharm.* **2017**, *113*, 178−187.
(78) Park, C. W.; Yang, H.-M.; Woo, M.-A.; Lee, K. S.; Kim, J.-D. Completely disintegrable redox-responsive poly (amino acid) nanogels for intracellular drug delivery. *J. Ind. Eng. Chem.* **2017**, *45*, 182−188.
(79) Krisch, E.; Messager, L.; Gyarmati, B.; Ravaine, V.; Szilágyi, A. Redox-and pH-Responsive Nanogels Based on Thiolated Poly (aspartic acid). *Macromol. Mater. Eng.* **2016**, *301* (3), 260−266.
(80) Gyarmati, B.; Némethy, Á.; Szilágyi, A. Reversible response of poly (aspartic acid) hydrogels to external redox and pH stimuli. *RSC Adv.* **2014**, *4* (17), 8764−8771.
(81) Krisch, E.; Gyarmati, B.; Barczikai, D.; Lapeyre, V.; Szilágyi, B. Á.; Ravaine, V.; Szilágyi, A. Poly (aspartic acid) hydrogels showing reversible volume change upon redox stimulus. *Eur. Polym. J.* **2018**, *105*, 459−468.
(82) Duggan, S.; Cummins, W.; O'Donovan, O.; Hughes, H.; Owens, E. Thiolated polymers as mucoadhesive drug delivery systems. *Eur. J. Pharm. Sci.* **2017**, *100*, 64−78.
(83) Budai-Szücs, M.; Horvát, G.; Gyarmati, B.; Szilágyi, B. Á.; Szilagyi, A.; Csihi, T.; Berkó, S.; Szabó-Révész, P.; Mori, M.; Sandri, G.; et al. In vitro testing of thiolated poly (aspartic acid) from ophthalmic formulation aspects. *Drug Dev. Ind. Pharm.* **2016**, *42* (8), 1241−1246.
(84) Budai-Szucs, M.; Kiss, E.; Szilagyi, B.; Szilagyi, A.; Gyarmati, B.; Berko, S.; Kovacs, A.; Horvat, G.; Aigner, Z.; Soos, J.; Csanyi, E. Mucoadhesive cyclodextrin-modified thiolated poly (aspartic acid) as a potential ophthalmic drug delivery system. *Polymers* **2018**, *10* (2), 199.
(85) Das, P.; Jana, N. R. Dopamine functionalized polymeric nanoparticle for targeted drug delivery. *RSC Adv.* **2015**, *5* (42), 33586−33594.
(86) Nakato, T.; Tomida, M.; Suwa, M.; Morishima, Y.; Kusuno, A.; Kakuchi, T. Preparation and characterization of dodecylamine-modified poly (aspartic acid) as a biodegradable water-soluble polymeric material. *Polym. Bull.* **2000**, *44* (4), 385−391.
(87) Xing, R.; Zhang, F.; Xie, J.; Aronova, M.; Zhang, G.; Guo, N.; Huang, X.; Sun, X.; Liu, G.; Bryant, L. H.; et al. Polyaspartic acid coated manganese oxide nanoparticles for efficient liver MRI. *Nanoscale* **2011**, *3* (12), 4943−4945.
(88) Yang, H.-M.; Oh, B. C.; Kim, J. H.; Ahn, T.; Nam, H.-S.; Park, C. W.; Kim, J.-D. Multifunctional poly (aspartic acid) nanoparticles containing iron oxide nanocrystals and doxorubicin for simultaneous cancer diagnosis and therapy. *Colloids Surf., A* **2011**, *391* (1−3), 208−215.
(89) Dong, X.; Lin, L.; Chen, J.; Tian, H.; Xiao, C.; Guo, Z.; Li, Y.; Wei, Y.; Chen, X. Multi-armed poly (aspartate-g-OEI) copolymers as versatile carriers of pDNA/siRNA. *Acta Biomater.* **2013**, *9* (6), 6943−6952.
(90) Zakeri, A.; Kouhbanani, M. A. J.; Beheshtkhoo, N.; Beigi, V.; Mousavi, S. M.; Hashemi, S. A. R.; Karimi Zade, A.; Amani, A. M.; Savardashtaki, A.; Mirzaei, E.; et al. Polyethylenimine-based nanocarriers in co-delivery of drug and gene: a developing horizon. *Nano reviews & experiments* **2018**, *9* (1), 1488497.
(91) Yeh, J.-C.; Yang, H.-H.; Hsu, Y.-T.; Su, C.-M.; Lee, T.-H.; Lou, S.-L. Synthesis and characteristics of biodegradable and temperature responsive polymeric micelles based on poly (aspartic acid)-g-poly (N-isopropylacrylamide-co-N, N-dimethylacrylamide). *Colloids Surf., A* **2013**, *421*, 1−8.
(92) Turecek, P. L.; Bossard, M. J.; Schoetens, F.; Ivens, I. A. PEGylation of biopharmaceuticals: a review of chemistry and nonclinical safety information of approved drugs. *J. Pharm. Sci.* **2016**, *105* (2), 460−475.
(93) Thuy, V. T. T.; Lim, C. W.; Park, J. H.; Ahn, C.-H.; Kim, D. Self-assembled nanoaggregates based on polyaspartamide graft copolymers for pH-controlled release of doxorubicin. *J. Mater. Chem. B* **2015**, *3* (15), 2978−2985.
(94) Chen, W.; Chen, H.; Hu, J.; Yang, W.; Wang, C. Synthesis and characterization of polyion complex micelles between poly (ethylene glycol)-grafted poly (aspartic acid) and cetyltrimethyl ammonium bromide. *Colloids Surf., A* **2006**, *278* (1−3), 60−66.
(95) Ryu, J. H.; Hong, S.; Lee, H. Bio-inspired adhesive catechol-conjugated chitosan for biomedical applications: A mini review. *Acta Biomater.* **2015**, *27*, 101−115.
(96) An, J. H.; Huynh, N. T.; Sil Jeon, Y.; Kim, J. H. Surface modification using bio-inspired adhesive polymers based on polyaspartamide derivatives. *Polym. Int.* **2011**, *60* (11), 1581−1586.
(97) Krogsgaard, M.; Nue, V.; Birkedal, H. Mussel-Inspired Materials: Self-Healing through Coordination Chemistry. *Chem. - Eur. J.* **2016**, *22* (3), 844−857.
(98) Vatankhah-Varnosfaderani, M.; Hu, X.; Li, Q.; Adelnia, H.; Ina, M.; Sheiko, S. S. Universal coatings based on zwitterionic-dopamine copolymer microgels. *ACS Appl. Mater. Interfaces* **2018**, *10* (24), 20869−20875.
(99) Vatankhah-Varnoosfaderani, M.; Ina, M.; Adelnia, H.; Li, Q.; Zhushma, A. P.; Hall, L. J.; Sheiko, S. S. Well-defined zwitterionic microgels: synthesis and application as acid-resistant microreactors. *Macromolecules* **2016**, *49* (19), 7204−7210.
(100) Gong, C.; Lu, C.; Li, B.; Shan, M.; Wu, G. Dopamine-modified poly (amino acid): an efficient near-infrared photothermal therapeutic agent for cancer therapy. *J. Mater. Sci.* **2017**, *52* (2), 955−967.
(101) Wang, B.; Kang, Y.; Shen, T.-Z.; Song, J.-K.; Park, H. S.; Kim, J.-H. Ultralight and compressible mussel-inspired dopamine-conjugated poly (aspartic acid)/Fe 3+-multifunctionalized graphene aerogel. *J. Mater. Sci.* **2018**, *53* (24), 16484−16499.
(102) Wang, B.; Jeon, Y. S.; Park, H. S.; Kim, J.-H. Self-healable mussel-mimetic nanocomposite hydrogel based on catechol-containing polyaspartamide and graphene oxide. *Mater. Sci. Eng., C* **2016**, *69*, 160−170.
(103) An, J. H.; Huynh, N. T.; Sil Jeon, Y.; Kim, J. H. J. P. I. Surface modification using bio-inspired adhesive polymers based on polyaspartamide derivatives. *Polym. Int.* **2011**, *60* (11), 1581−1586.
(104) Lu, Y.; Chau, M.; Boyle, A.; Liu, P.; Niehoff, A.; Weinrich, D.; Reilly, R. M.; Winnik, M. A. Effect of pendant group structure on the hydrolytic stability of polyaspartamide polymers under physiological conditions. *Biomacromolecules* **2012**, *13* (5), 1296−1306.
(105) Nakato, T.; Yoshitake, M.; Matsubara, K.; Tomida, M.; Kakuchi, T. Relationships between structure and properties of poly (aspartic acid) s. *Macromolecules* **1998**, *31* (7), 2107−2113.

https://doi.org/10.1021/acsbiomaterials.1c00150
ACS Biomater. Sci. Eng. XXXX, XXX, XXX−XXX

(106) Alford, D. D.; Wheeler, A.; Pettigrew, C. A. Biodegradation of thermally synthesized polyaspartate. *J. Environ. Polym. Degrad.* **1994**, *2* (4), 225−236.
(107) Tabata, K.; Abe, H.; Doi, Y. Microbial Degradation of Poly (aspartic acid) by Two Isolated Strains of Pedobacter sp. and Sphingomonas sp. *Biomacromolecules* **2000**, *1* (2), 157−161.
(108) Tabata, K.; Kajiyama, M.; Hiraishi, T.; Abe, H.; Yamato, I.; Doi, Y. Purification and characterization of poly (aspartic acid) hydrolase from Sphingomonas sp. KT-1. *Biomacromolecules* **2001**, *2* (4), 1155−1160.
(109) Yu-Ling, Z.; Zhi-Guang, H.; Jiao-Long, W.; Qian, L.; Jun-Li, H. Biodegradation of poly (aspartic acid-lysine) copolymers by mixed bacteria from natural water. *Polym. Degrad. Stab.* **2016**, *128*, 134−140.
(110) Wei, J.; Xue, M.; Li, C.; Cao, H.; Tan, T. Effect of enzyme and mechanical stirring on the degradation of polyaspartic acid Hydro-gel. *Prog. Nat. Sci.* **2015**, *25* (5), 425−429.
(111) Yang, J.; Wang, F.; Tan, T. Degradation behavior of hydrogel based on crosslinked poly (aspartic acid). *J. Appl. Polym. Sci.* **2010**, *117* (1), 178−185.
(112) Zhang, C.; Wu, S.; Wu, J.; Wu, D.; Qin, X. Preparation and characterization of microporous sodium poly (aspartic acid) nanofibrous hydrogel. *J. Porous Mater.* **2017**, *24* (1), 75−84.
(113) Juriga, D. V.; Nagy, K.; Jedlovszky-Hajdú, A. L.; Perczel-Kovách, K.; Chen, Y. M.; Varga, G. B.; Zrínyi, M. S. Biodegradation and osteosarcoma cell cultivation on poly (aspartic acid) based hydrogels. *ACS Appl. Mater. Interfaces* **2016**, *8* (36), 23463−23476.
(114) Hayashi, T.; Iwatsuki, M. Biodegradation of copoly (L-aspartic acid/L-glutamic acid) in vitro. *Biopolymers* **1990**, *29* (3), 549−557.
(115) Juriga, D.; Zrínyi, M. In *Biodegradation of Poly (aspartamide) Based Hydrogels*; Macromolecular Symposia; Wiley: 2019; p 1800194.
(116) Salakhieva, D. V.; Gumerova, D.; Akhmadishina, R.; Kamalov, M.; Nizamov, I.; Nemeth, C.; Szilágyi, A.; Abdullin, T. Anti-Radical and Cytotoxic Activity of Polysuccinimide and Polyaspartic Acid of Different Molecular Weight. *BioNano Science* **2016**, *6* (4), 348−351.
(117) Juriga, D. V.; Nagy, K.; Jedlovszky-Hajdú, A. L.; Perczel-Kovách, K.; Chen, Y. M.; Varga, G. B.; Zrínyi, M. Biodegradation and osteosarcoma cell cultivation on poly (aspartic acid) based hydrogels. *ACS Appl. Mater. Interfaces* **2016**, *8* (36), 23463−23476.
(118) Kim, H. J.; Kim, U.-J.; Kim, H. S.; Li, C.; Wada, M.; Leisk, G. G.; Kaplan, D. L. Bone tissue engineering with premineralized silk scaffolds. *Bone* **2008**, *42* (6), 1226−1234.
(119) Zhou, M.; Hou, T.; Li, J.; Yu, S.; Xu, Z.; Yin, M.; Wang, J.; Wang, X. Self-propelled and targeted drug delivery of poly (aspartic acid)/iron-zinc microrocket in the stomach. *ACS Nano* **2019**, *13* (2), 1324−1332.
(120) Sadeghiani, N.; Barbosa, L.; Silva, L.; Azevedo, R.; Morais, P.; Lacava, Z. Genotoxicity and inflammatory investigation in mice treated with magnetite nanoparticles surface coated with polyaspartic acid. *J. Magn. Magn. Mater.* **2005**, *289*, 466−468.
(121) Juriga, D.; Sipos, E.; Hegedüs, O.; Varga, G.; Zrínyi, M.; Nagy, K. S.; Jedlovszky-Hajdú, A. Fully amino acid-based hydrogel as potential scaffold for cell culturing and drug delivery. *Beilstein J. Nanotechnol.* **2019**, *10* (1), 2579−2593.
(122) Sharma, S.; Anwar, M. F.; Dinda, A.; Singhal, M.; Malik, A. In Vitro and in Vivo Studies of pH-Sensitive GHK-Cu-Incorporated Polyaspartic and Polyacrylic Acid Superabsorbent Polymer. *ACS omega* **2019**, *4* (23), 20118−20128.
(123) Lu, C.; Zhao, D.; Wang, S.; Wang, Y.; Wang, Y.; Gao, H.; Ma, J.; Wu, G. Synthesis and characterization of zwitterionic peptides derived from natural amino acids and their resistance to protein adsorption. *RSC Adv.* **2014**, *4* (40), 20665−20672.
(124) Lim, S.; Nguyen, M. P.; Choi, Y.; Kim, J.; Kim, D. Bioadhesive nanoaggregates based on polyaspartamide-g-C18/DOPA for wound healing. *Biomacromolecules* **2017**, *18* (8), 2402−2409.
(125) Wan, J.; Sun, L.; Wu, P.; Wang, F.; Guo, J.; Cheng, J.; Wang, C. Synthesis of indocyanine green functionalized comblike poly (aspartic acid) derivatives for enhanced cancer cell ablation by targeting the endoplasmic reticulum. *Polym. Chem.* **2018**, *9* (10), 1206−1215.
(126) Jiang, B.; Liu, M.; Zhang, K.; Zu, G.; Dong, J.; Cao, Y.; Zhang, L.; Pei, R. Oligoethylenimine grafted PEGylated poly (aspartic acid) as a macromolecular contrast agent: properties and in vivo studies. *J. Mater. Chem. B* **2016**, *4* (19), 3324−3330.
(127) Abbasian, M.; Massoumi, B.; Mohammad-Rezaei, R.; Samadian, H.; Jaymand, M. Scaffolding polymeric biomaterials: Are naturally occurring biological macromolecules more appropriate for tissue engineering? *Int. J. Biol. Macromol.* **2019**, *134*, 673.
(128) Niu, X.; Wang, Y.; Xu, C.; Fu, Z.; Bai, S.; Wang, J.; Wang, Y.; Guo, X. Access to Highly Tough Hydrogels by Polymer Modules for Application of Catalytic Reactors. *Ind. Eng. Chem. Res.* **2020**, *59* (11), 4977−4986.
(129) Bakht Khosh Hagh, H.; Farshi Azhar, F. Reinforcing materials for polymeric tissue engineering scaffolds: A review. *J. Biomed. Mater. Res., Part B* **2019**, *107* (5), 1560−1575.
(130) Ghafari, R.; Jonoobi, M.; Amirabad, L. M.; Oksman, K.; Taheri, A. R. Fabrication and characterization of novel bilayer scaffold from nanocellulose based aerogel for skin tissue engineering applications. *Int. J. Biol. Macromol.* **2019**, *136*, 796−803.
(131) Jang, J.; Cha, C. Multivalent polyaspartamide cross-linker for engineering cell-responsive hydrogels with degradation behavior and tunable physical properties. *Biomacromolecules* **2018**, *19* (2), 691−700.
(132) Asati, S.; Pandey, V.; Soni, V. RGD peptide as a targeting moiety for theranostic purpose: An update study. *Int. J. Pept. Res. Ther.* **2019**, *25* (1), 49−65.
(133) Sharifzadeh, G.; Soheilmoghaddam, M.; Adelnia, H.; Wahit, M. U.; Arzhandi, M. R. D.; Moslehyani, A. Biocompatible regenerated cellulose/halloysite nanocomposite fibers. *Polym. Eng. Sci.* **2020**, *60*, 1169.
(134) Molnar, K.; Juriga, D.; Nagy, P. M.; Sinko, K.; Jedlovszky-Hajdu, A.; Zrinyi, M. Electrospun poly (aspartic acid) gel scaffolds for artificial extracellular matrix. *Polym. Int.* **2014**, *63* (9), 1608−1615.
(135) Stroganov, V.; Pant, J.; Stoychev, G.; Janke, A.; Jehnichen, D.; Fery, A.; Handa, H.; Ionov, L. 4D biofabrication: 3D cell patterning using shape-changing films. *Adv. Funct. Mater.* **2018**, *28* (11), 1706248.
(136) Gooding, J. J. Finally, a simple solution to biofouling. *Nat. Nanotechnol.* **2019**, *14* (12), 1089−1090.
(137) Wang, X.; Wu, G.; Lu, C.; Wang, Y.; Fan, Y.; Gao, H.; Ma, J. Synthesis of a novel zwitterionic biodegradable poly (α, β-L-aspartic acid) derivative with some L-histidine side-residues and its resistance to non-specific protein adsorption. *Colloids Surf., B* **2011**, *86* (1), 237−241.
(138) Xu, M.; Zhao, Y.; Feng, M. Polyaspartamide derivative nanoparticles with tunable surface charge achieve highly efficient cellular uptake and low cytotoxicity. *Langmuir* **2012**, *28* (31), 11310−11318.
(139) Qiu, W.-Z.; Yang, H.-C.; Xu, Z.-K. Dopamine-assisted co-deposition: an emerging and promising strategy for surface modification. *Adv. Colloid Interface Sci.* **2018**, *256*, 111−125.
(140) Sudheer, P. Mucoadhesive polymers: A review. *J. Pharmaceut. Res.* **2018**, *17* (1), 47−55.
(141) Ramasamy, T.; Munusamy, S.; Ruttala, H. B.; Kim, J. O. Smart Nanocarriers for the Delivery of Nucleic Acid-based Therapeutics: A Comprehensive Review. *Biotechnol. J.* **2020**, 1900408.
(142) Shen, J.; Zhao, D.; Li, W.; Hu, Q.; Wang, Q.; Xu, F.; Tang, G. A polyethylenimine-mimetic biodegradable polycation gene vector and the effect of amine composition in transfection efficiency. *Biomaterials* **2013**, *34* (18), 4520−4531.
(143) Licciardi, M.; Campisi, M.; Cavallaro, G.; Carlisi, B.; Giammona, G. Novel cationic polyaspartamide with covalently linked carboxypropyl-trimethyl ammonium chloride as a candidate vector for gene delivery. *Eur. Polym. J.* **2006**, *42* (4), 823−834.
(144) Dou, X.; Hu, Y.; Zhao, N.; Xu, F. Different types of degradable vectors from low-molecular-weight polycation-functionalized poly (aspartic acid) for efficient gene delivery. *Biomaterials* **2014**, *35* (9), 3015−3026.

https://doi.org/10.1021/acsbiomaterials.1c00150
ACS Biomater. Sci. Eng. XXXX, XXX, XXX−XXX

(145) Itaka, K.; Ishii, T.; Hasegawa, Y.; Kataoka, K. Biodegradable polyamino acid-based polycations as safe and effective gene carrier minimizing cumulative toxicity. *Biomaterials* **2010**, *31* (13), 3707−3714.
(146) Zhang, M.; Liu, M.; Xue, Y.-N.; Huang, S.-W.; Zhuo, R.-X. Polyaspartamide-based oligo-ethylenimine brushes with high buffer capacity and low cytotoxicity for highly efficient gene delivery. *Bioconjugate Chem.* **2009**, *20* (3), 440−446.
(147) Salakhieva, D.; Shevchenko, V.; Németh, C.; Gyarmati, B.; Szilágyi, A.; Abdullin, T. Structure-biocompatibility and transfection activity relationships of cationic polyaspartamides with (dialkylamino) alkyl and alkyl or hydroxyalkyl side groups. *Int. J. Pharm.* **2017**, *517* (1−2), 234−246.
(148) Ma, C.; Zhang, J.; Guo, L.; Du, C.; Song, P.; Zhao, B.; Li, L.; Li, C.; Qiao, R. Cyclen Grafted with poly [(Aspartic acid)-co-Lysine]: Preparation, Assembly with Plasmid DNA, and in Vitro Transfection Studies. *Mol. Pharmaceutics* **2016**, *13* (1), 47−54.
(149) Li, C.; Tian, H.; Rong, N.; Liu, K.; Liu, F.; Zhu, Y.; Qiao, R.; Jiang, Y. Chitosan grafted with macrocyclic polyamines on C-2 and C-6 positions as nonviral gene vectors: Preparation, characterization, and in vitro transfection studies. *Biomacromolecules* **2011**, *12* (2), 298−305.
(150) Yavvari, P. S.; Verma, P.; Mustfa, S. A.; Pal, S.; Kumar, S.; Awasthi, A. K.; Ahuja, V.; Srikanth, C.; Srivastava, A.; Bajaj, A. A nanogel based oral gene delivery system targeting SUMOylation machinery to combat gut inflammation. *Nanoscale* **2019**, *11* (11), 4970−4986.
(151) Kim, F.; Chen, T.; Burgess, T.; Rasie, P.; Selinger, T. L.; Greschner, A.; Rizis, G.; Carneiro, K. Functionalized DNA nanostructures as scaffolds for guided mineralization. *Chemical Science* **2019**, *10* (45), 10537−10542.
(152) Lee, E. S.; Kim, J. H.; Sim, T.; Youn, Y. S.; Lee, B.-J.; Oh, Y. T.; Oh, K. T. A feasibility study of a pH sensitive nanomedicine using doxorubicin loaded poly (aspartic acid-graft-imidazole)-block-poly (ethylene glycol) micelles. *J. Mater. Chem. B* **2014**, *2* (9), 1152−1159.
(153) Hatamihanza, H.; Alavi, S. E.; Shahmabadi, H. E.; Akbarzadeh, A. Preparation, Characterization and Immunostimulatory Effects of CRD2 and CRD3 from TNF Receptor-1 Encapsulated into Pegylated Liposomal Nanoparticles. *Int. J. Peptide Res. Therapeut.* **2019**, 1−9.
(154) Koohi Moftakhari Esfahani, M.; Alavi, S. E.; Shahbazian, S.; Ebrahimi Shahmabadi, H. Drug Delivery of Cisplatin to Breast Cancer by Polybutylcyanoacrylate Nanoparticles. *Adv. Polym. Technol.* **2018**, *37* (3), 674−678.
(155) Al Harthi, S.; Alavi, S. E.; Radwan, M. A.; El Khatib, M. M.; AlSarra, I. A. Nasal delivery of donepezil HCl-loaded hydrogels for the treatment of Alzheimer's disease. *Sci. Rep.* **2019**, *9*, 9563.
(156) Alavi, S. E.; Cabot, P. J.; Moyle, P. M. Glucagon-Like Peptide-1 Receptor Agonists and Strategies To Improve Their Efficiency. *Mol. Pharmaceutics* **2019**, *16* (6), 2278−2295.
(157) Ibie, C.; Knott, R.; Thompson, C. Complexation of novel thiomers and insulin to protect against in vitro enzymatic degradation-towards oral insulin delivery. *Drug Dev. Ind. Pharm.* **2019**, *45* (1), 67−75.
(158) Sattari, S.; Dadkhah Tehrani, A.; Adeli, M.; Azarbani, F. Development of new nanostructure based on poly (aspartic acid)-g-amylose for targeted curcumin delivery using helical inclusion complex. *J. Mol. Liq.* **2018**, *258*, 18−26.
(159) Wan, S.; Huang, J.; Guo, M.; Zhang, H.; Cao, Y.; Yan, H.; Liu, K. Biocompatible superparamagnetic iron oxide nanoparticle dispersions stabilized with poly (ethylene glycol)-oligo (aspartic acid) hybrids. *J. Biomed. Mater. Res., Part A* **2007**, *80* (4), 946−954.
(160) Golabdar, A.; Adelnia, H.; Moshtzan, N.; Nasrollah Gavgani, J.; Izadi-Vasafi, H. Anti-bacterial poly (vinyl alcohol) nanocomposite hydrogels reinforced with in situ synthesized silver nanoparticles. *Polym. Compos.* **2019**, *40* (4), 1322−1328.
(161) Vazquez-Prada, K. X.; Lam, J.; Kamato, D.; Ping Xu, Z.; Little, P. J.; Ta, H. T. Targeted Molecular Imaging of Cardiovascular Diseases by Iron Oxide Nanoparticles. *Arterioscler. Thromb. Vasc. Biol.* **2021**, *41*, 601−613.
(162) Arndt, N.; Tran, H. D. N.; Zhang, R.; Xu, Z. P.; Ta, H. T. Different Approaches to Develop Nanosensors for Diagnosis of Diseases. *Adv. Sci. (Weinh)* **2020**, *7* (24), 2001476.
(163) Zia, A.; Wu, Y.; Nguyen, T.; Wang, X.; Peter, K.; Ta, H. T. The choice of targets and ligands for site-specific delivery of nanomedicine to atherosclerosis. *Cardiovasc. Res.* **2020**, *116* (13), 2055−2068.
(164) Liu, Y.; Wu, Y.; Zhang, R.; Lam, J.; Ng, J. C.; Xu, Z. P.; Li, L.; Ta, H. T. Investigating the Use of Layered Double Hydroxide Nanoparticles as Carriers of Metal Oxides for Theranostics of ROS-Related Diseases. *ACS Appl. Bio Mater.* **2019**, *2* (12), 5930−5940.
(165) Yusof, N. N. M.; McCann, A.; Little, P. J.; Ta, H. T. J. T. R. Non-invasive imaging techniques for the differentiation of acute and chronic thrombosis. *Thromb. Res.* **2019**, *177*, 161−171.
(166) Yamashita, S.; Katsumi, H.; Hibino, N.; Isobe, Y.; Yagi, Y.; Tanaka, Y.; Yamada, S.; Naito, C.; Yamamoto, A. Development of PEGylated aspartic acid-modified liposome as a bone-targeting carrier for the delivery of paclitaxel and treatment of bone metastasis. *Biomaterials* **2018**, *154*, 74−85.
(167) Ta, H. T.; Li, Z.; Wu, Y.; Cowin, G.; Zhang, S.; Yago, A.; Whittaker, A. K.; Xu, Z. P. J. M. R. E. Effects of magnetic field strength and particle aggregation on relaxivity of ultra-small dual contrast iron oxide nanoparticles. *Mater. Res. Express* **2017**, *4* (11), 116105.
(168) Ta, H.; Prabhu, S.; Leitner, E.; Jia, F.; Putnam, K.; Bassler, N.; Peter, K.; Hagemeyer, C. J. A. Targeted molecular imaging and cell homing in cardiovascular disease via antibody-sortagging. *Atherosclerosis* **2015**, *241* (1), No. e26.
(169) Ta, H. T.; Prabhu, S.; Leitner, E.; Jia, F.; Putnam, K.; Bassler, N.; Peter, K.; Hagemeyer, C. Antibody-sortagging: a universal approach towards targeted molecular imaging and cell homing in cardiovascular disease. *Circ. Res.* **2010**, *107* (12), No. e37-e38.
(170) Ta, H. T.; Arndt, N.; Wu, Y.; Lim, H. J.; Landeen, S.; Zhang, R.; Kamato, D.; Little, P. J.; Whittaker, A. K.; Xu, Z. P. J. N. Activatable magnetic resonance nanosensor as a potential imaging agent for detecting and discriminating thrombosis. *Nanoscale* **2018**, *10* (31), 15103−15115.
(171) Ta, H.; Li, Z.; Hagemeyer, C.; Cowin, G.; Palasubramaniam, J.; Peter, K.; Whittaker, A. J. A. Self-confirming molecular imaging of activated platelets via iron oxide nanoparticles displaying unique dual MRI contrast. *Atherosclerosis* **2017**, *263*, No. e146.
(172) Khandekar, S. V.; Kulkarni, M.; Devarajan, P. V. Polyaspartic acid functionalized gold nanoparticles for tumor targeted doxorubicin delivery. *J. Biomed. Nanotechnol.* **2014**, *10* (1), 143−153.
(173) Jalalvandi, E.; Hanton, L. R.; Moratti, S. C. Schiff-base based hydrogels as degradable platforms for hydrophobic drug delivery. *Eur. Polym. J.* **2017**, *90*, 13−24.
(174) Némethy, Á.; Solti, K.; Kiss, L.; Gyarmati, B.; Deli, M. A.; Csányi, E.; Szilágyi, A. pH-and temperature-responsive poly (aspartic acid)-l-poly (N-isopropylacrylamide) conetwork hydrogel. *Eur. Polym. J.* **2013**, *49* (9), 2392−2403.
(175) Budai-Szucs, M.; Kiss, E.; Szilagyi, B.; Szilagyi, A.; Gyarmati, B.; Berko, S.; Kovacs, A.; Horvat, G.; Aigner, Z.; Soos, J.; Csanyi, E. Mucoadhesive Cyclodextrin-Modified Thiolated Poly (aspartic acid) as a Potential Ophthalmic Drug Delivery System. *Polymers* **2018**, *10* (2), 199.
(176) Lu, J.; Li, Y.; Hu, D.; Chen, X.; Liu, Y.; Wang, L.; Zhao, Y. Synthesis and properties of pH-, thermo-, and salt-sensitive modified poly (aspartic acid)/poly (vinyl alcohol) IPN hydrogel and its drug controlled release. *BioMed. Res. Int.* **2015**, *2015*, 236745.
(177) Cheng, X.; Liu, J.; Wang, L.; Wang, R.; Liu, Z.; Zhuo, R. An enzyme-mediated in situ hydrogel based on polyaspartamide derivatives for localized drug delivery and 3D scaffolds. *RSC Adv.* **2016**, *6* (103), 101334−101346.
(178) Sattari, S.; Dadkhah Tehrani, A.; Adeli, M.; Azarbani, F. Development of new nanostructure based on poly (aspartic acid)-g-amylose for targeted curcumin delivery using helical inclusion complex. *J. Mol. Liq.* **2018**, *258*, 18−26.

https://doi.org/10.1021/acsbiomaterials.1c00150
ACS Biomater. Sci. Eng. XXXX, XXX, XXX−XXX

(179) Gu, X.; Wang, J.; Wang, Y.; Wang, Y.; Gao, H.; Wu, G. Layer-by-layer assembled polyaspartamide nanocapsules for pH-responsive protein delivery. *Colloids Surf., B* **2013**, *108*, 205−211.
(180) Yuan, Y.; Zhao, L.; Shen, C.; He, Y.; Yang, F.; Zhang, G.; Jia, M.; Zeng, R.; Li, C.; Qiao, R. Reactive oxygen species-responsive amino acid-based polymeric nanovehicles for tumor-selective anticancer drug delivery. *Materi Sci. Eng., C* **2019**, *106*, 110159.
(181) Chastain, D. B.; Davis, A. Treatment of chronic osteomyelitis with multidose oritavancin: A case series and literature review. *Int. J. Antimicrob. Agents* **2019**, *53* (4), 429−434.
(182) Hasson, D.; Shemer, H.; Sher, A. State of the art of friendly "green" scale control inhibitors: a review article. *Ind. Eng. Chem. Res.* **2011**, *50* (12), 7601−7607.
(183) Ogawa, K.; Ishizaki, A.; Takai, K.; Kitamura, Y.; Kiwada, T.; Shiba, K.; Odani, A. Development of novel radiogallium-labeled bone imaging agents using oligo-aspartic acid peptides as carriers. *PLoS One* **2013**, *8* (12), No. e84335.
(184) Wang, D.; Miller, S. C.; Shlyakhtenko, L. S.; Portillo, A. M.; Liu, X.-M.; Papangkorn, K.; Kopecková, P.; Lyubchenko, Y.; Higuchi, W. I.; Kopeček, J. Osteotropic peptide that differentiates functional domains of the skeleton. *Bioconjugate Chem.* **2007**, *18* (5), 1375−1378.
(185) Liu, J.; Zeng, Y.; Shi, S.; Xu, L.; Zhang, H.; Pathak, J. L.; Pan, Y. Design of polyaspartic acid peptide-poly (ethylene glycol)-poly (ε-caprolactone) nanoparticles as a carrier of hydrophobic drugs targeting cancer metastasized to bone. *Int. J. Nanomed.* **2017**, *12*, 3561.
(186) Giachelli, C. M.; Speer, M. Y.; Li, X.; Rajachar, R. M.; Yang, H. Regulation of vascular calcification: roles of phosphate and osteopontin. *Circ. Res.* **2005**, *96* (7), 717−722.
(187) Icer, M. A.; Gezmen-Karadag, M. The multiple functions and mechanisms of osteopontin. *Clin. Biochem.* **2018**, *59*, 17−24.

https://doi.org/10.1021/acsbiomaterials.1c00150
ACS Biomater. Sci. Eng. XXXX, XXX, XXX−XXX